Biomaterials dedicated to bone regeneration

SNOSCELLS
Les Houches

Pierre Weiss
INSERM U 1229
RMES Regenerative medicine and skeleton,
University of Nantes, 1 place Alexis Ricordeau, 44042 Nantes, France.
E-mail : pierre.weiss@univ-nantes.fr

Day 2

Regenerative biomaterials for bone

- Biomaterials in bone regenerative medicine.

Biomaterials for bone regeneration

- **Autogenous bone (Gold Standard)**
  - Limited bone stock (small packs)
  - High risk of morbidity
  - Painful and not aesthetic

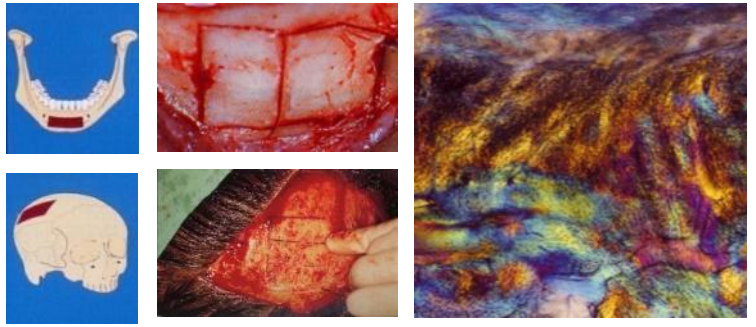

- **Allograft (Human)**
- **Xenograft bone (Animal)**
  - Infection (bacterial - viral)
  - Dead bones limit cell proliferation
  - Legal requirements (biological origins)

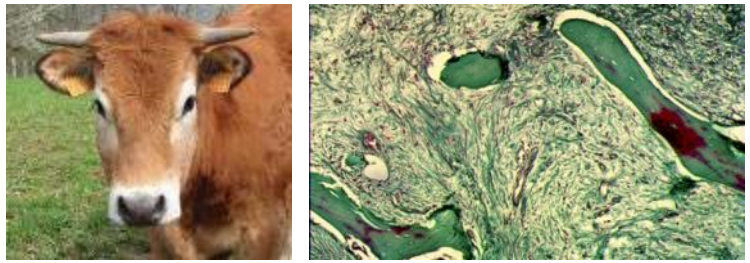

- **Calcium Phosphates**
  - Wide variety on the market
  - Different quality and clinical results
  - Very specific production know-how

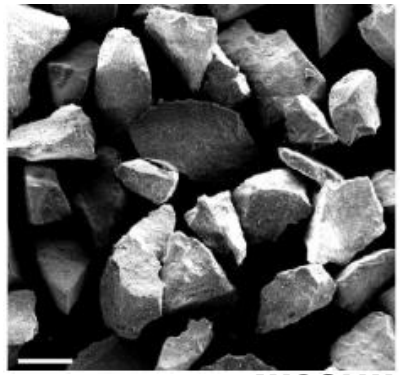

- **Bio Glasses**
  - Controlled synthetic material
  - Able to recruit osteoprogenitor cells, the "stem cells" of bone.
  - controls the cycle of osteoblasts to promote proliferation and differentiation

Biomaterial Design

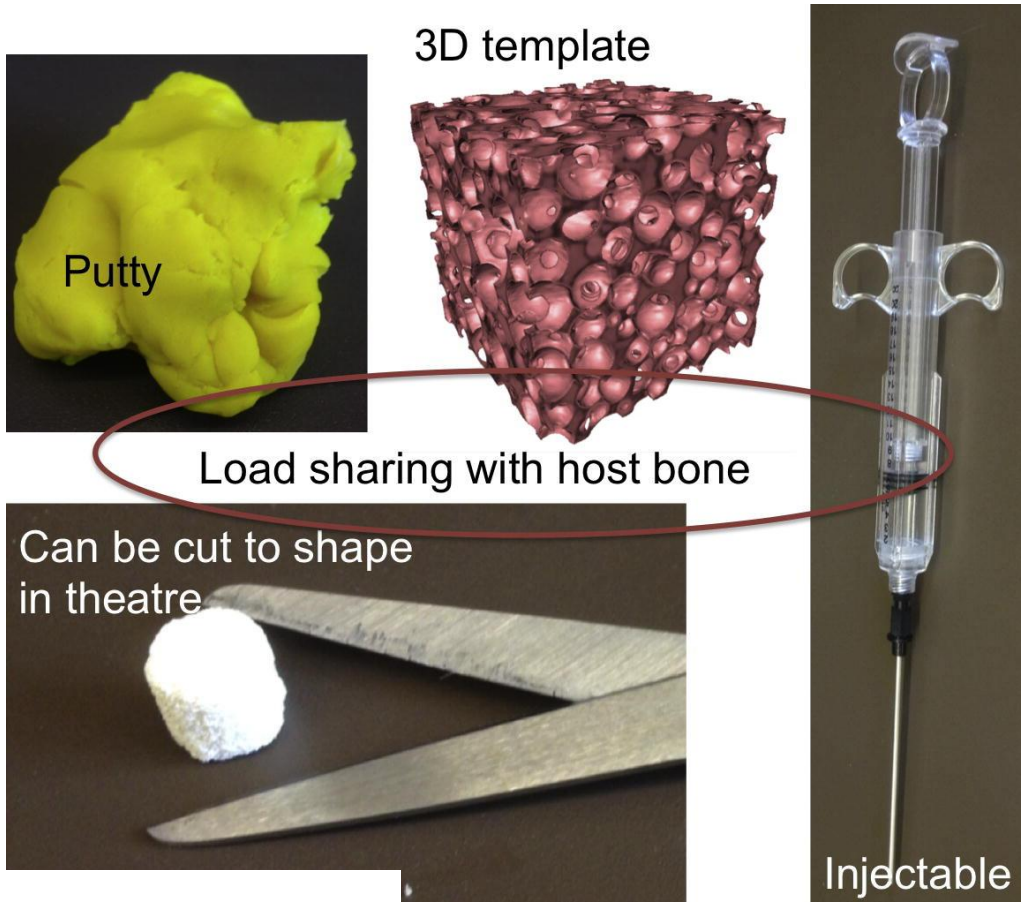

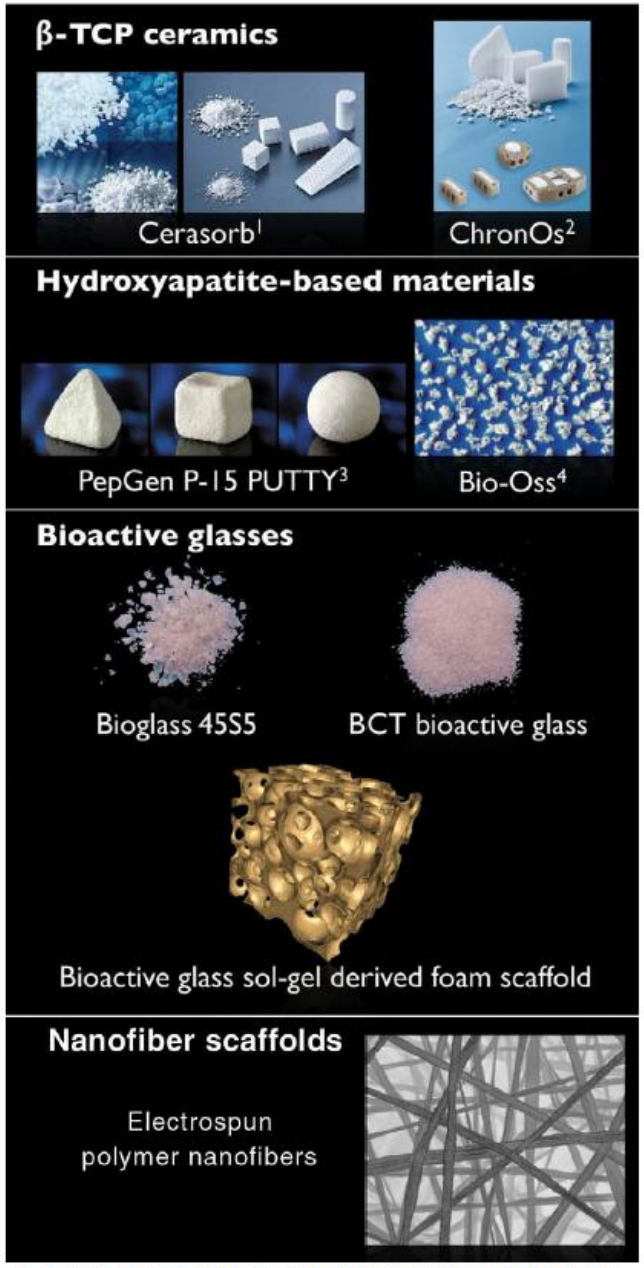

Fig. 2. Macromorphology of some examples of different bone graft materials. (Reproduced with permission from [1]Curasan AG, [2]Synthes, [4]Geistlich. [3]Courtesy of Dentsply Tulsa Dental Specialties. © PepGen® P-15.)

Acta Biomaterialia 23 (2015) S53–S82
Contents lists available at ScienceDirect
Acta Biomaterialia
journal homepage: www.elsevier.com/locate/actabiomat

Review

Reprint of: Review of bioactive glass: From Hench to hybrids

Julian R. Jones *
Department of Materials, Imperial College London, South Kensington Campus, London SW7 2AZ, UK

Calcium Phosphate pionniers

Biological and synthetic apatites

Bone mineral:

$Ca_{8,3}\ (PO_4)_{4,3}\ (HPO_4,CO_3)_{1,7}\ (OH,CO_3)_{0,3}$

Dental enamel Mineral:

$Ca_{9,4}\ (PO_4)_{5,4}\ (HPO_4,CO_3)_{0,6}\ (OH,CO_3)_{1,4}$

Hydroxyapatite

$Ca_{10}\ (P0_4)_6\ (OH)_2$

Beta Tricalcique Phosphate (β-TCP) :

$Ca_3\ (P04)_2$

Biphasic calcium phosphate BCP = HA + β-TCP

Monocalcium Phosphate

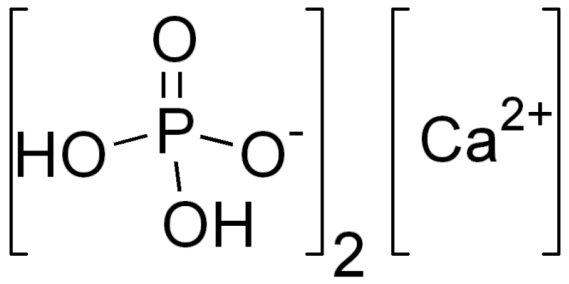

Dicalcium phosphate

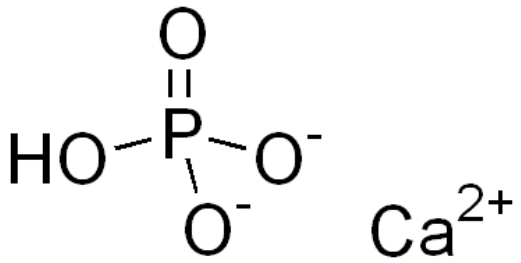

tricalcium Phosphate : TCP :

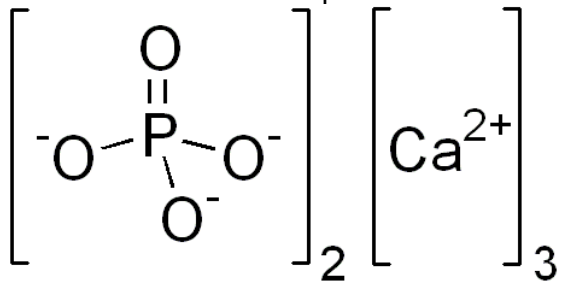

Table 1
Existing calcium orthophosphates and their major properties [21,22].

Ca/P molar ratio	Compound	Formula	Solubility at 25 °C, -log(K_s)	Solubility at 25 °C, g/L	pH stability range in aqueous solutions at 25 °C
0.5	Monocalcium phosphate monohydrate (MCPM)	$Ca(H_2PO_4)_2 \cdot H_2O$	1.14	~18	0.0–2.0
0.5	Monocalcium phosphate anhydrous (MCPA)	$Ca(H_2PO_4)_2$	1.14	~17	[c]
1.0	Dicalcium phosphate dihydrate (DCPD), mineral brushite	$CaHPO_4 \cdot 2H_2O$	6.59	~0.088	2.0–6.0
1.0	Dicalcium phosphate anhydrous (DCPA), mineral monetite	$CaHPO_4$	6.90	~0.048	[c]
1.33	Octacalcium phosphate (OCP)	$Ca_8(HPO_4)_2(PO_4)_4 \cdot 5H_2O$	96.6	~0.0081	5.5–7.0
1.5	α-Tricalcium phosphate (α-TCP)	$\alpha\text{-}Ca_3(PO_4)_2$	25.5	~0.0025	[a]
1.5	β-Tricalcium phosphate (β-TCP)	$\beta\text{-}Ca_3(PO_4)_2$	28.9	~0.0005	[a]
1.2–2.2	Amorphous calcium phosphate (ACP)	$Ca_xH_y(PO_4)_z \cdot nH_2O$, $n = 3–4.5$; 15–20% H_2O	[b]	[b]	~5–12[d]
1.5–1.67	Calcium-deficient hydroxyapatite (CDHA)[e]	$Ca_{10-x}(HPO_4)_x(PO_4)_{6-x}(OH)_{2-x}$[f] $(0 < x < 1)$	~85.1	~0.0094	6.5–9.5
1.67	Hydroxyapatite (HA or OHAp)	$Ca_{10}(PO_4)_6(OH)_2$	116.8	~0.0003	9.5–12
1.67	Fluorapatite (FA or FAp)	$Ca_{10}(PO_4)_6F_2$	120.0	~0.0002	7–12
2.0	Tetracalcium phosphate (TTCP or TetCP), mineral hilgenstockite	$Ca_4(PO_4)_2O$	38–44	~0.0007	[a]

CA

[a] These compounds cannot be precipitated from aqueous solutions.
[b] Cannot be measured precisely. However, the following values were found: 25.7 ± 0.1 (pH = 7.40), 29.9 ± 0.1 (pH = 6.00), 32.7 ± 0.1 (pH = 5.28). The comparative extent of dissolution in acidic buffer is: ACP >> α-TCP >> β-TCP > CDHA >> HA > FA.
[c] Stable at temperatures above 100 °C.
[d] Always metastable.
[e] Occasionally, CDHA is named as precipitated HA.
[f] In the case $x = 1$ (the boundary condition with Ca/P = 1.5), the chemical formula of CDHA looks as follows: $Ca_9(HPO_4)(PO_4)_5(OH)$.

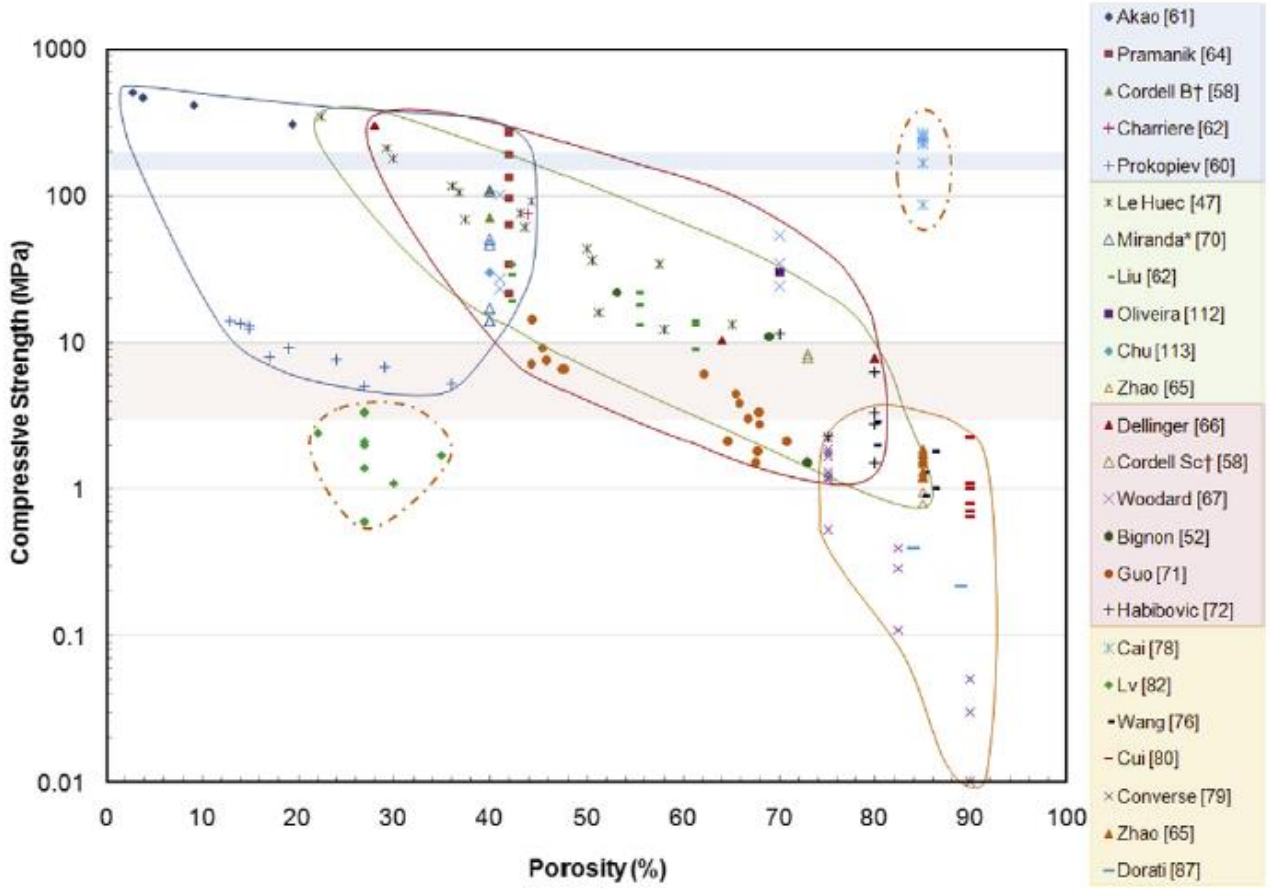

Fig. 2. Plot illustrating the dependence of compressive strength on total porosity for all references included in Fig. 1. The data are grouped by material category using colored lines. Bulk HA and BCP, HA scaffolds, BCP scaffolds, HA/polymer and polymer scaffolds are represented by blue, green, red and orange lines, respectively. One exception is Miranda et al. (denoted by *). These data are included in the BCP category, but are the only study in that category with β-TCP and no HA. Two data sets from two different groups are considered "outliers" and are demarcated with dashed lines. Table 2 is also the legend to this figure.

Biological activity of CaP

Table 3
Overview of porosity, pore size and biological properties.

Product name	Porosity (%)	Pore size (μm)	Osteogenic	Osteoinductive	Osteoconductive	Biodegradable
Calcium phosphate						
Hydroxyapatite						
Cerabone®	N.D.	(100–1500)	N.D.	N.D.	Yes [47]	N.D.
Endobon®	60–80 [24]	390–1360 [22]	N.D.	No [38]	Yes [24,38,41,43,44,65,82,83,159,160]	No [39–44]
Ostim®	N.D.	N.D.	N.D.	N.D.	Yes [45–50,85,161,162]	Yes [45–50]
Pro Osteon 500®	N.D.	(280–770)	N.D.	N.D.	Yes [40,163,164]	No [165]
Tricalcium phosphate						
ChronOS™	60–75 [25,27,28]	100–400 [25,28]	N.D.	N.D.	Yes [25,27,166–168]	Yes [27,167,169]
Vitoss®	(88–92)	(1–1000)	N.D.	N.D.	Yes [25,170]	Yes [25]
Composite						
BoneSave®	(50)	(300–500)	N.D.	N.D.	N.D.	N.D.
BoneSource®	46 [29,30]	2–50 [31]	N.D.	Yes [29]	Yes [30,72,74,110,171–176]	Yes [72,171,172,174,175]
Calcibon®	30–40 [32,33]	<1 [33]	N.D.	No [37]	Yes [33,37,57,177,178]	Yes [57,179,180]
Camceram®	N.D.	N.D.	N.D.	N.D.	N.D.	N.D.
ChronOS™ Inject	N.D.	N.D.	N.D.	N.D.	Yes [58,62,181]	Yes [58,62,181]
HydroSet™	N.D.	N.D.	N.D.	N.D.	N.D.	N.D.
norian SRS®	(50)	N.D.	N.D.	N.D.	Yes [59–63,95]	Yes [59–62]/no [63]
Calcium sulphate						
Bone Plast®	N.D.	N.D.	N.D.	N.D.	N.D.	N.D.
MIIG® X3	N.D.	N.D.	N.D.	N.D.	Yes [117–119]	Yes [117–119]
OsteoSet®	N.D.	N.D.	N.D.	N.D.	Yes [120–123]/no [124,125]	Yes [120–125,128]
Stimulan®	N.D.	N.D.	N.D.	N.D.	N.D.	N.D.
Bioactive glass						
Cortoss®	(1)	N.D.	N.D.	N.D.	Yes [139]	Yes [140]

Data obtained from the suppliers are given between brackets.
N.D., no data available.

Calcium Phosphate Ceramics

Céramique = cohésion de la structure assurés par traitement thermique

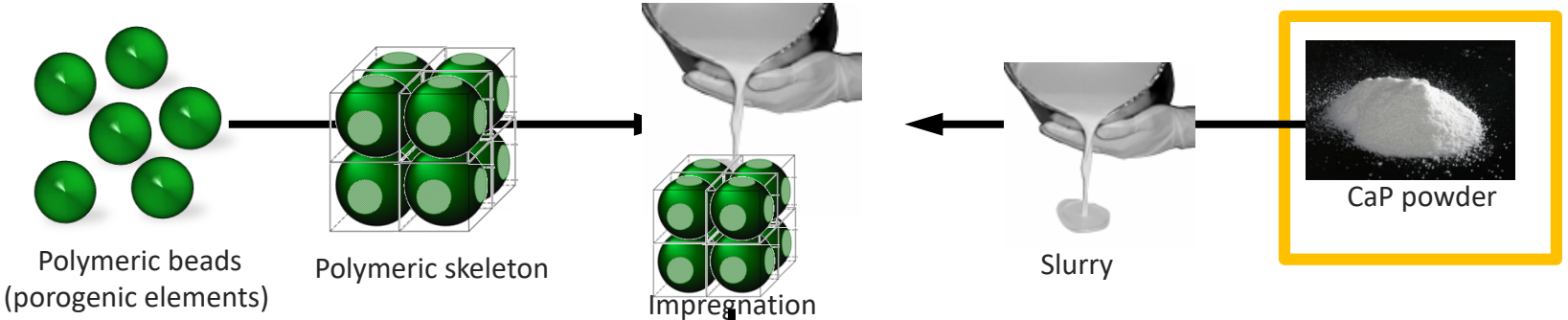

Drying

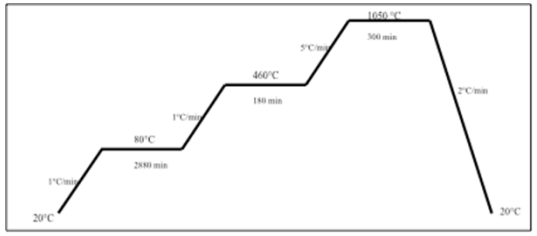

"Green" 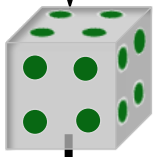 = Polymeric skeleton + CaP

Thermal treatment (debinding then sintering)

Porous Ceramic 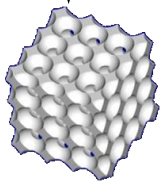 = Bone substitute

Calcium phosphate ceramics biomaterials

Sinter the powders

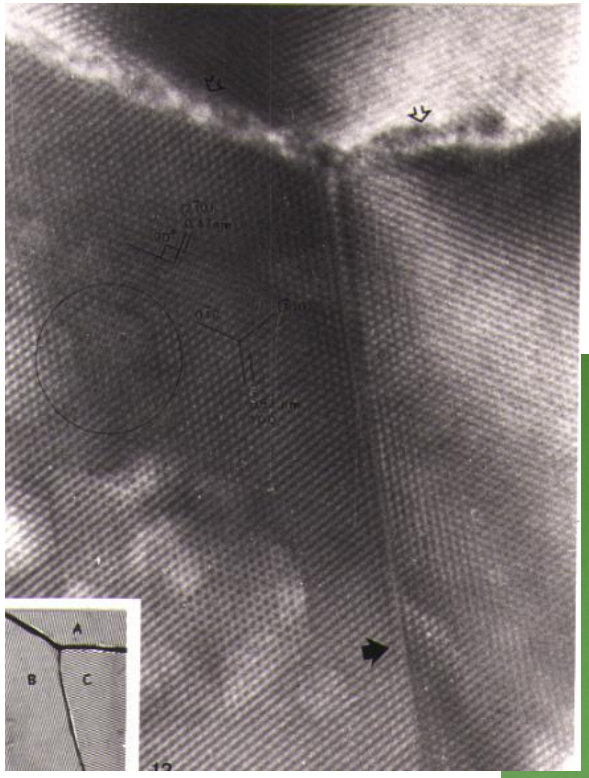

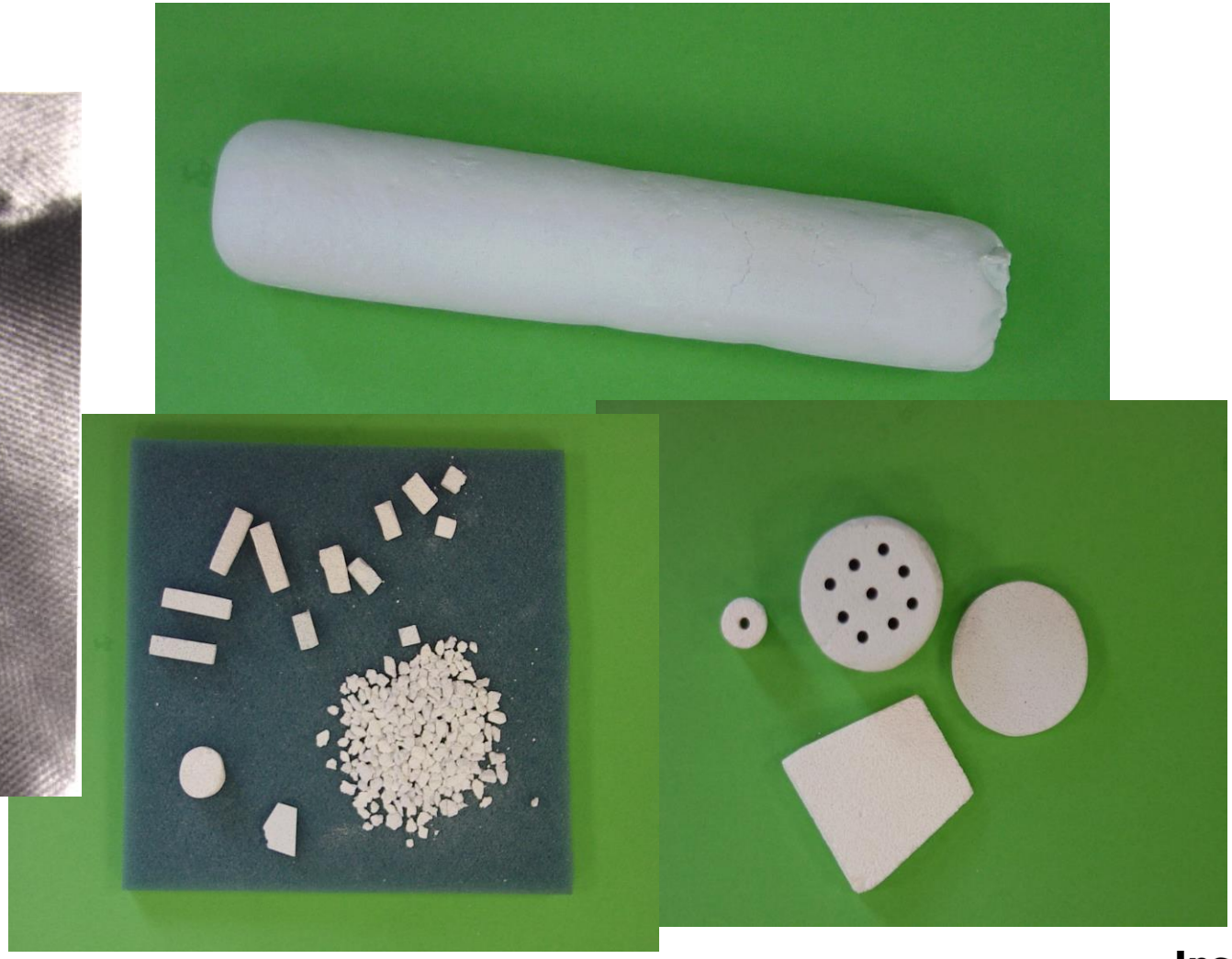

Porosity

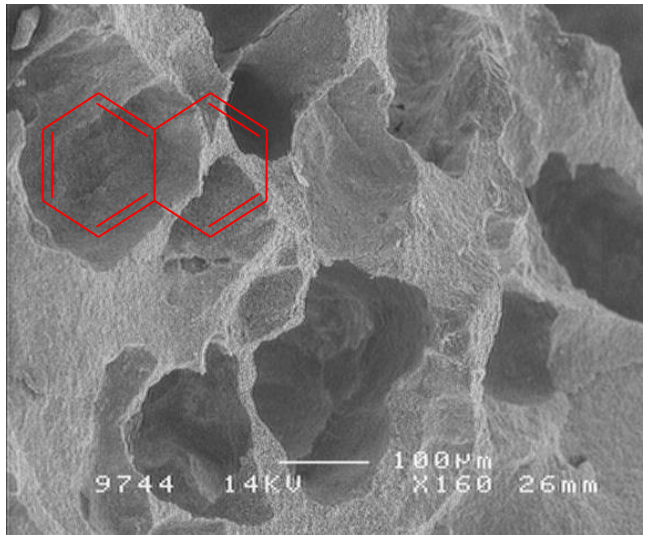

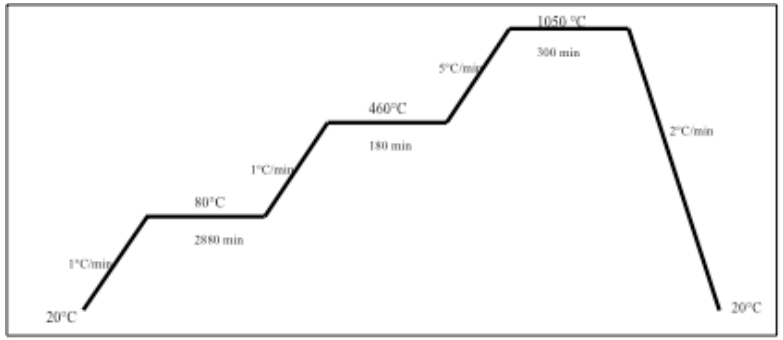

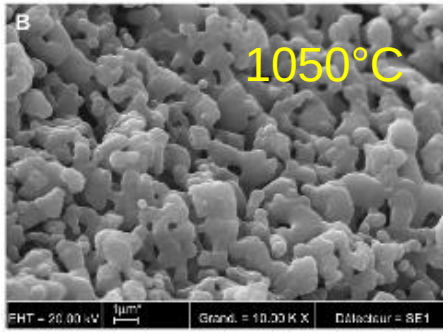

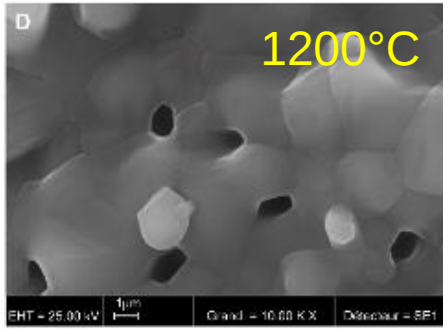

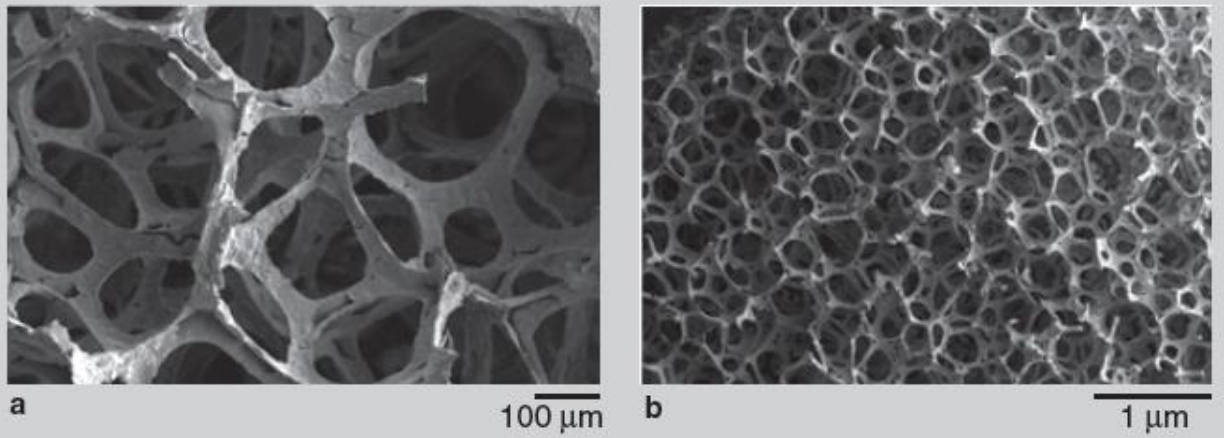

Figure 3. Porous hydroxyapatite produced through replication of a reticulated polymer foam.

Journal of Non-Crystalline Solids 432 (2016) 2–8

Contents lists available at ScienceDirect

Journal of Non-Crystalline Solids

journal homepage: www.elsevier.com/ locate/ jnoncrysol

Bioglass

Bioglass: 10 milestones from concept to commerce

Larry L. Hench

Department of Biomedical Engineering, Florida Institute of Technology, Melbourne, FL, USA

Table 1
Milestones of science and clinical product development of 45S5 Bioglass.

1971	First publication of bonding of bone to bioactive glasses and glass-ceramics
1981	Discovery of soft connective tissue bonding to 45S5 Bioglass
1981	Toxicology and biocompatibility studies (16 in vitro and in vivo) published to establish safety for FDA clearance of bioglass products
1985	First medical product (Bioglass Ossicular Reconstruction Prosthesis) (MEP) cleared by FDA via the 510 (k) process
1987	Discovery of osteostimulation in use of Bioglass particulate in regeneration of bone
1988	Bioglass Endosseous Ridge Maintenance Implant (ERMI) cleared by FDA via the 510 (k) process
1991	Development of sol–gel processing method for making bioactive gel-glasses extending the bioactive compositional range of bioactivity
1993	Bioglass particulate for use in bone grafting to restore bone loss from periodontal disease in infrabony defects (PerioGlas) cleared by FDA via the 510 (k) process
1996	Use of PerioGlas for bone grafts in tooth extraction sites and alveolar ridge augmentation cleared by FDA *via* the 510 (k) process
2000	FDA clearance for use of NovaBone in general orthopedic bone grafting in non-load bearing sites
2000	Quantitative comparison of rate of trabecular bone formation in presence of Bioglass granules versus synthetic HA and A/W glass-ceramic
2000	Analysis of use of 45S5 Bioglass ionic dissolution products to control osteoblast cell cycles
2001	Gene expression profiling of 45S5 Bioglass ionic dissolution products to enhance osteogenesis
2004	FDA clearance of 45S5 particulate for use in dentinal hypersensitivity treatment (NovaMin)

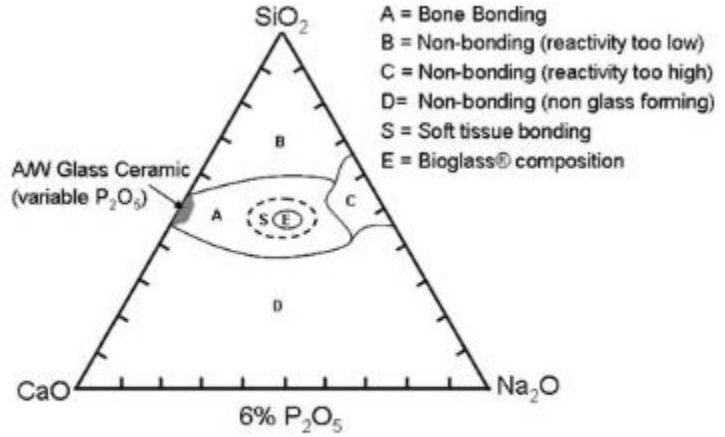

Fig. 1 Compositional diagram for bone-bonding. Note regions A, B, C, D. Region S is a region of Class A bioactivity where bioactive glasses bond to both bone and soft tissues and are gene activating

J Mater Sci: Mater Med (2006) 17:967–978
DOI 10.1007/s10856-006-0432-z

The story of Bioglass®

Larry L. Hench

Bio glass

Acta Biomaterialia 23 (2015) S53–S82

Contents lists available at ScienceDirect

Acta Biomaterialia

journal homepage: www.elsevier.com/locate/actabiomat

Review

Reprint of: Review of bioactive glass: From Hench to hybrids

Julian R. Jones *

Department of Materials, Imperial College London, South Kensington Campus, London SW7 2AZ, UK

«A glass is a non-crystalline solid exhibiting the glass transition phenomenon » (Zarzycki 1982)

Selected properties of melt-derived Bioglass 45S5 [60,148].

Property	Value
Density	2.7 g cm^{-3}
Network connectivity	2.12
Glass transition temperature	538 °C
Onset of crystallization	677 °C
Thermal expansion coefficient	15.1 × 10^{-6} $°C^{-1}$
Young's modulus (stiffness)	35 MPa

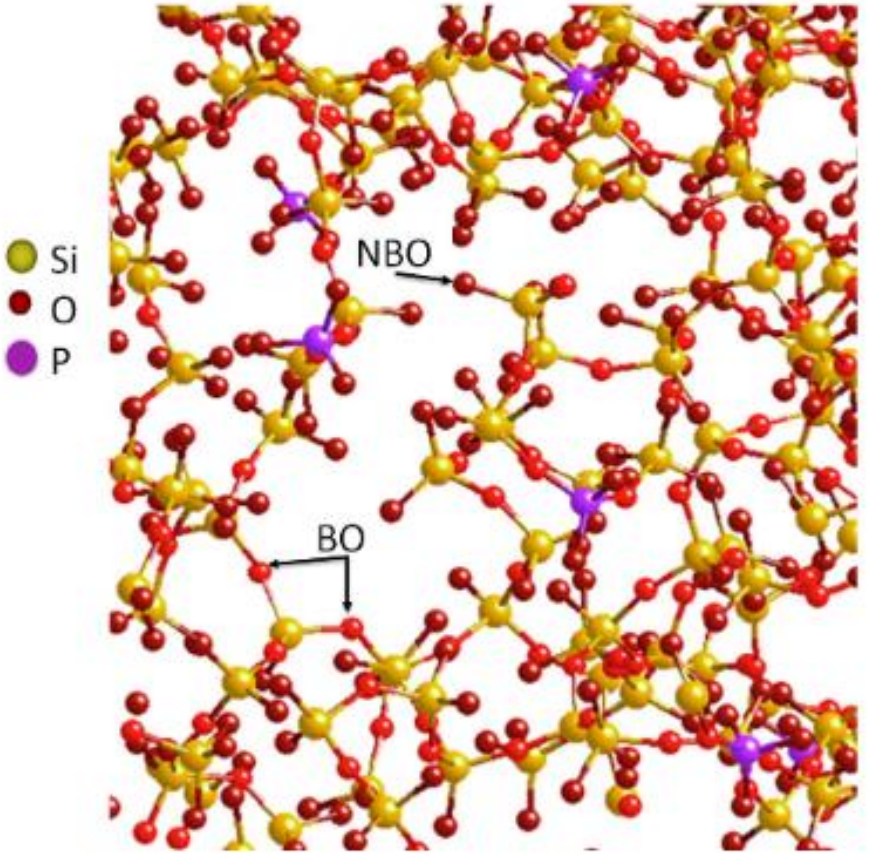

Fig. 10. Section of a model of Bioglass® 45S5, with the Na and Ca ions removed for clarity. NBO – non-bridging oxygen, BO – bridging oxygen. Modified from Cormack et al. [136].

Synthesis

Fusion : Mixture of inorganic raw materials heated between 1300 and 1600 °C then cooled without allowing crystallization

Sol-gel: A solution that gels by polymerizing in an aqueous medium. Then the gel is dried and heated

Structural transformations of bio-glasses:

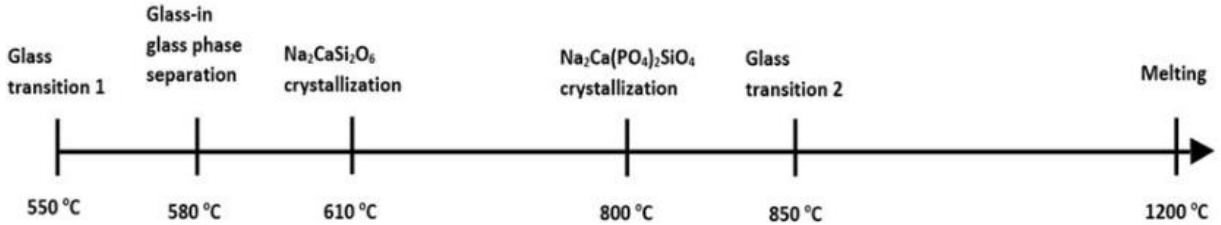

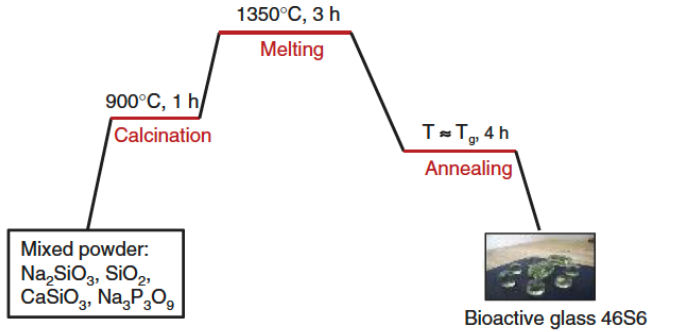

Figure 14 The thermal process for the synthesis of bioactive glass 46S6. Modified from Ref. [138].

DE GRUYTER

Review

Azizeh-Mitra Yousefi*, Hassane Oudadesse, Rosa Akbarzadeh, Eric Wers and Anita Lucas-Girot

Physical and biological characteristics of nanohydroxyapatite and bioactive glasses used for bone tissue engineering

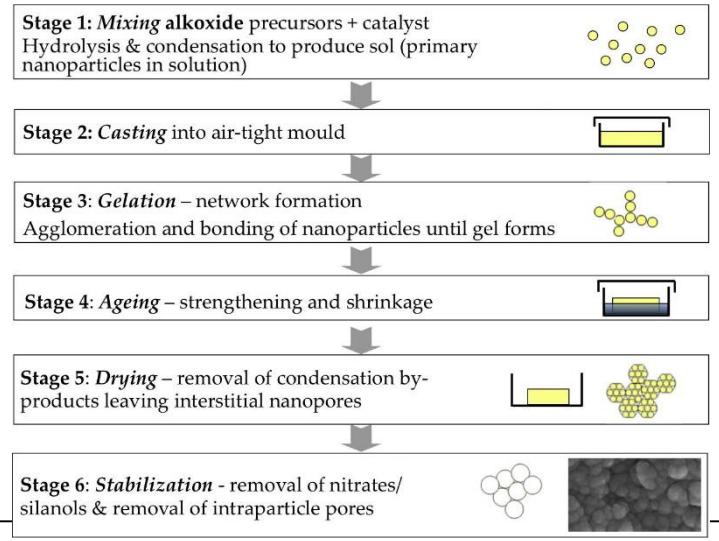

A flow chart of the acid-catalysed sol–gel process of synthesis of a bioactive glass with schematics of the evolution of the gel and its nanoporosity.

Differents Bio Glasses

- Particle size: Micro to nanometric
- Compositions: with Silver, Potassium, Magnesium, Strontium...
- Nano or meso porosity
- +/- Crystallized

Table IV. Composition of Bioactive Glasses and Glass-Ceramics (wt%)

Component	45S5 Bioglass®	45S5.4F Bioglass®	45B15S5 Bioglass®	52S4.6 Bioglass®	55S4.3 Bioglass®	KGC Ceravital®	KGS Ceravital®	KGy213 Ceravital®	A/W glass-ceramic	MB glass-ceramic	S45P7
SiO_2	45	45	30	52	55	46.2	46	38	34.2	19–52	45
P_2O_5	6	6	6	6	6				16.3	4–24	7
CaO	24.5	14.7	24.5	21	19.5	20.2	33	31	44.9	9–3	22
$Ca(PO_3)_2$						25.5	16	13.5			
CaF_2		9.8							0.5		
MgO						2.9			4.6	5–15	
MgF_2											
Na_2O	24.5	24.5	24.5	21	19.5	4.8	5	4		3–5	24
K_2O						0.4				3–5	
Al_2O_3								7		12–33	
B_2O_3			15								2
Ta_2O_5/TiO_2								6.5			
Structure	Glass and glass-ceramic	Glass	Glass	Glass		Glass-ceramic	Glass-ceramic	Glass-ceramic	Glass-ceramic	Glass-ceramic	

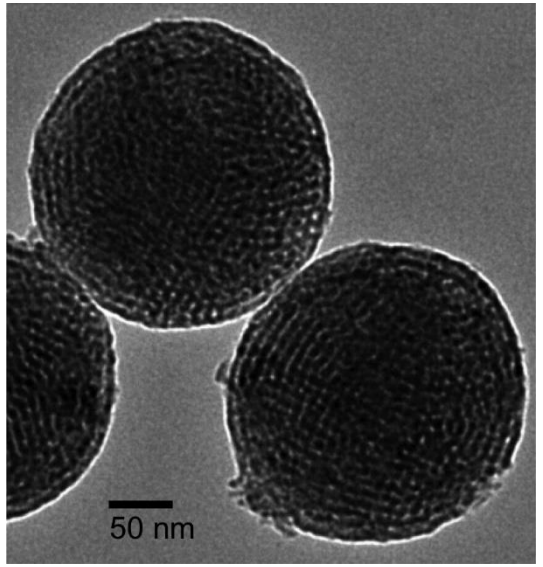

Transmission electron microscope image of ordered mesoporous silica particles. Courtesy of Lijun Ji, Yangzhou University, China.

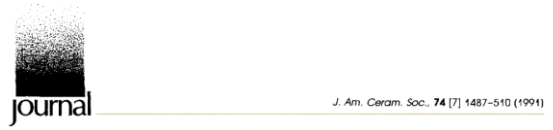

Journal of Non-Crystalline Solids 412 (2016) 2–8
Contents lists available at ScienceDirect
Journal of Non-Crystalline Solids
journal homepage: www.elsevier.com/locate/jnoncrysol

Bone regeneration with Bio Glass

Bioglass: 10 milestones from concept to commerce
Larry L Hench
Department of Biomedical Engineering, Florida Institute of Technology, Melbourne, FL, USA

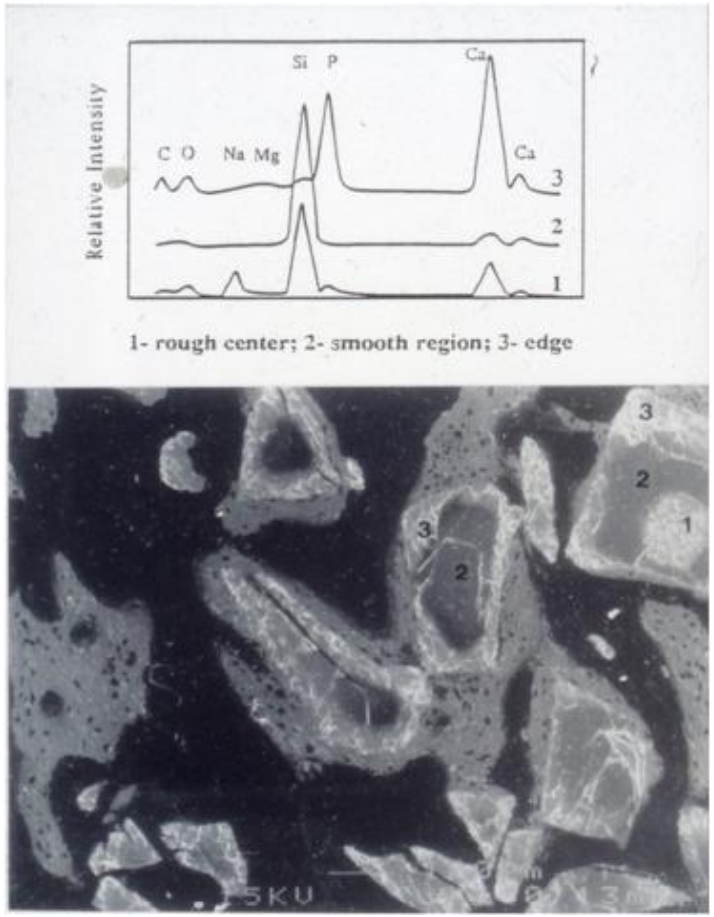

Scanning electron micrograph (SEM) of new bone growing around and connecting 45S5 Bioglass particles to form a regenerated trabecular bone structure. Upper figure is SEM-EDS analysis of the composition gradients of the Bioglass particles due to ion exchange reactions that lead to growth of a biologically active hydroxyl-carbonate-apatite (HCA) layer that is rich is in Ca, region #3.

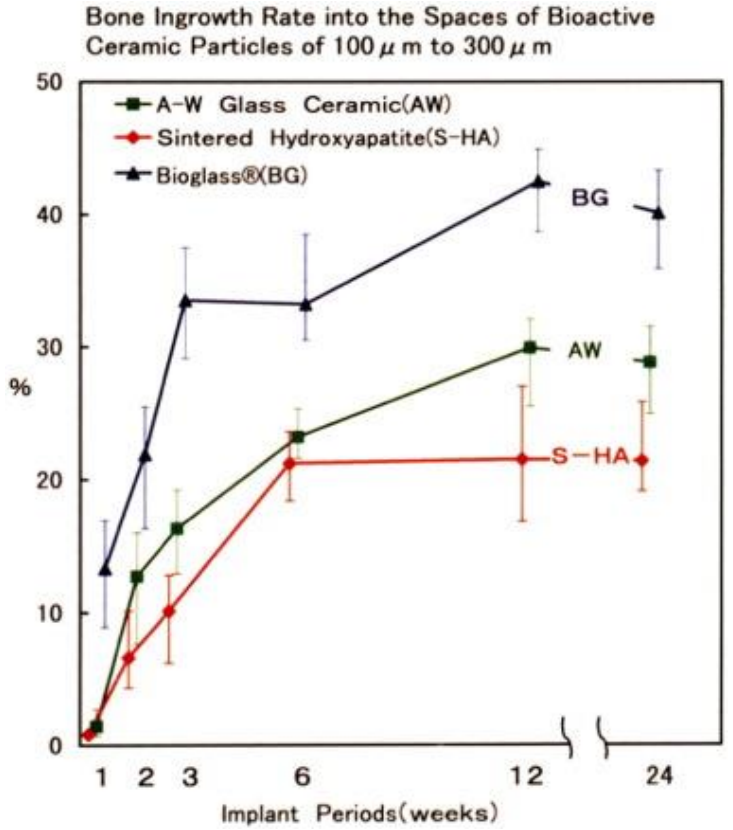

Rapid regeneration of new bone from Class A Bioglass versus Class B bioactive A/W and HA particles in Oonishi critical size defect rabbit condyle model. Note rapid growth of new bone within 4weeks in the presence of Bioglass particles and eventual greater amount of bone regenerated within the critical size defect.

Calcium Phosphate Suspensions in HPMC viscous water solution

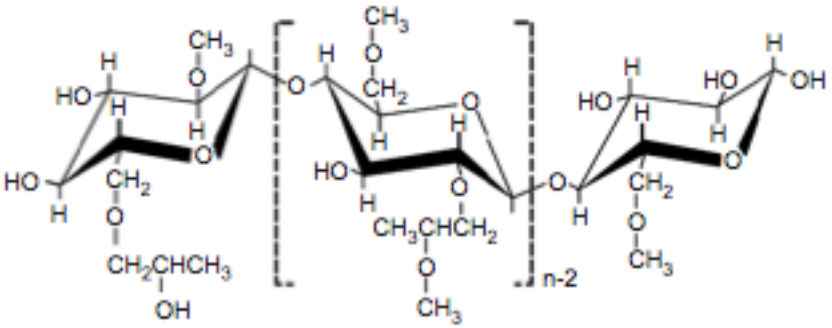

2% HPMC in water + BCP granules

WO 9521634 (A1) Injectable Bone Substitute : WEISS P, DACULSI G,, DELECRIN J, GRIMANDI G ET PASSUTI N

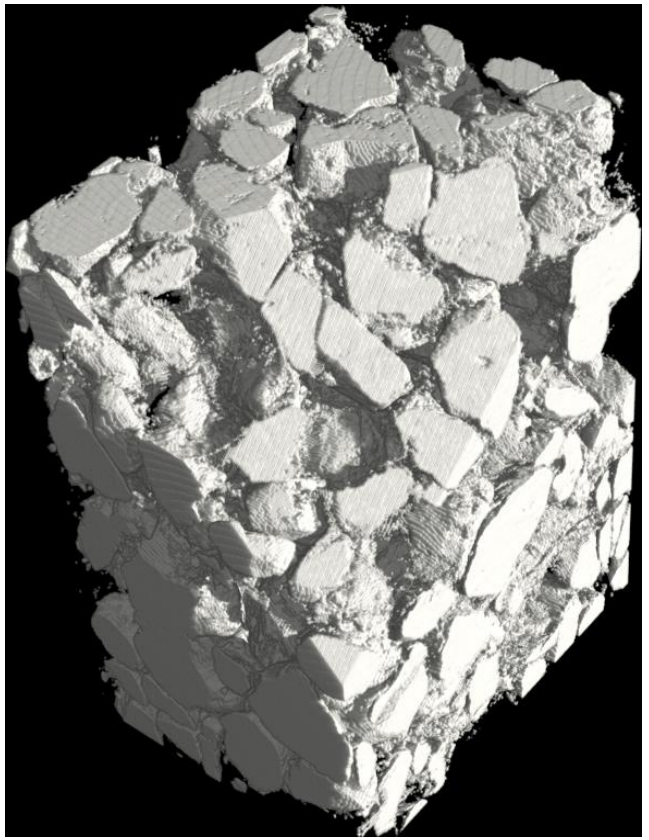

Without hardening properties

ELSEVIER

Available online at www.sciencedirect.com
ScienceDirect

Biomaterials 28 (2007) 3295–3305

Biomaterials

www.elsevier.com/locate/biomaterials

The safety and efficacy of an injectable bone substitute in dental sockets demonstrated in a human clinical trial

Pierre Weiss[a,b,c,*], Pierre Layrolle[a,b], Léon Philippe Clergeau[b,c], Bénédicte Enckel[b,c], Paul Pilet[a,c], Yves Amouriq[b,c], Guy Daculsi[a,b], Bernard Giumelli[b,c]

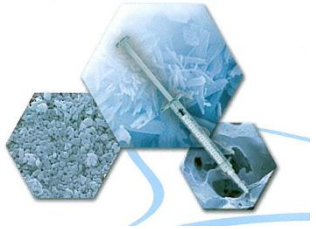

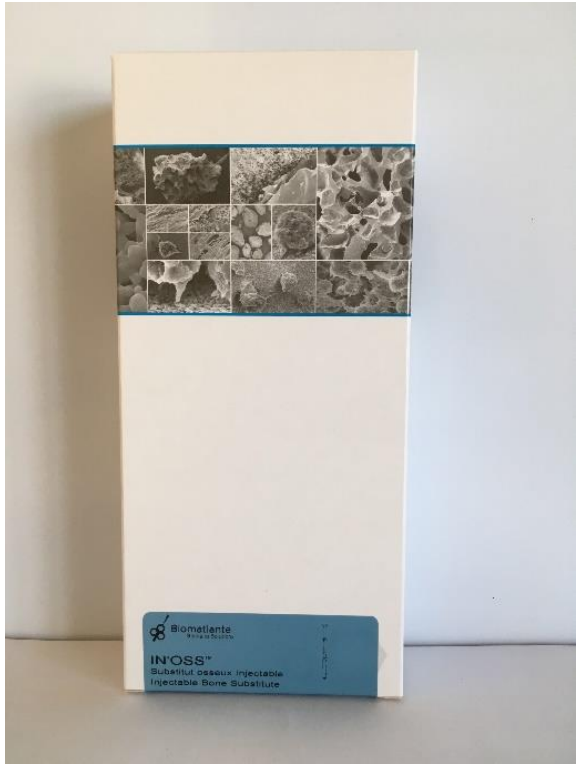

Cement

Cement (hydraulic) = structural cohesion provided by soft chemistry

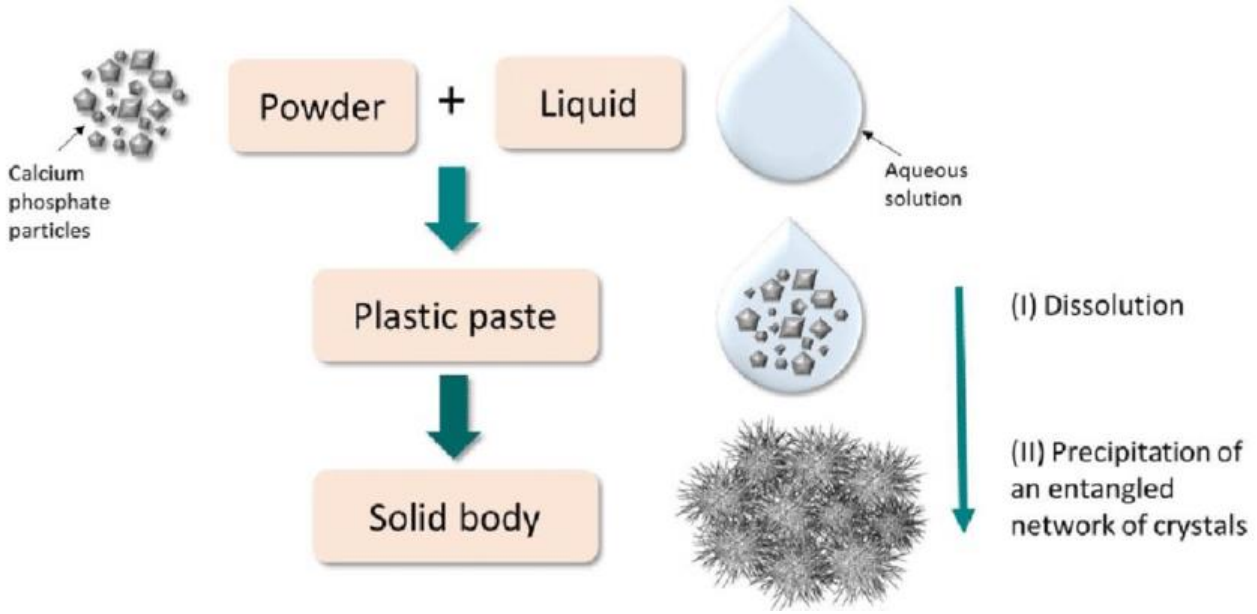

Cements


Injection
Prise

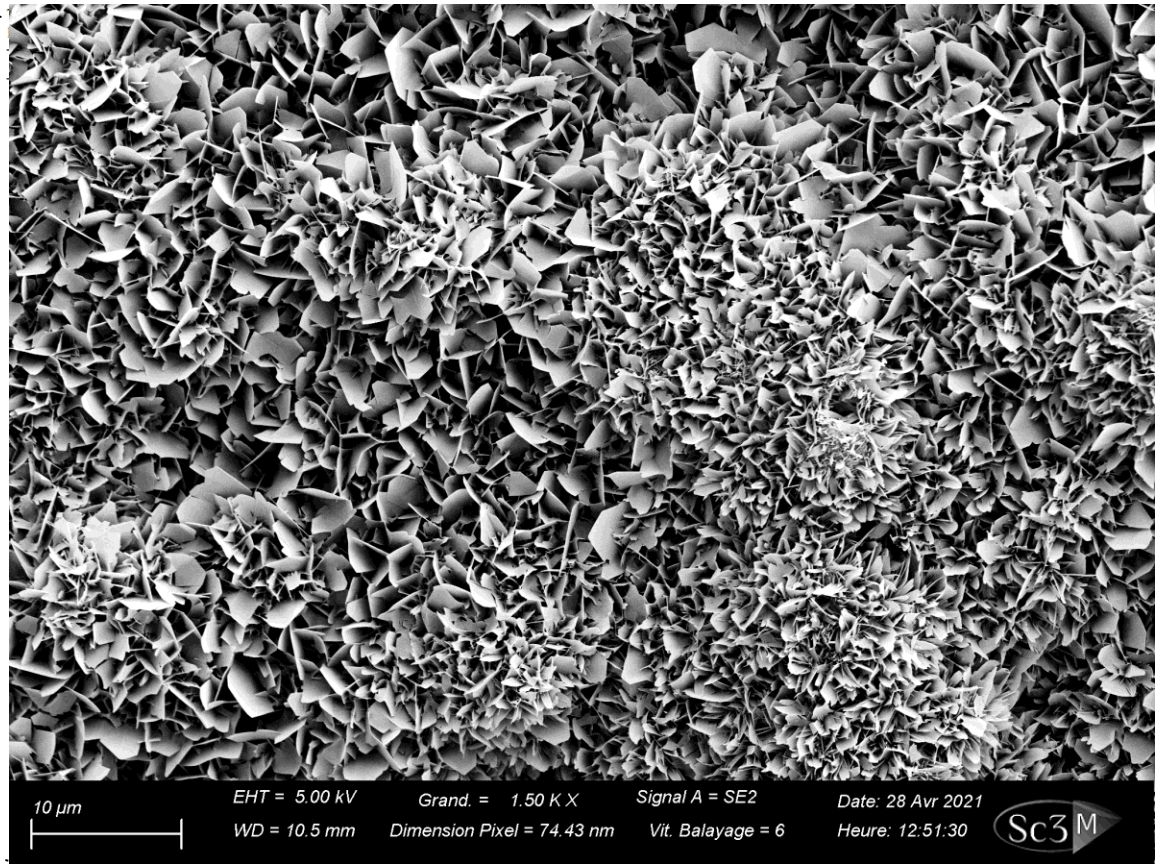
10 µm
EHT = 5.00 kV
WD = 10.5 mm
Grand. = 1.50 K X
Dimension Pixel = 74.43 nm
Signal A = SE2
Vit. Balayage = 6
Date: 28 Avr 2021
Heure: 12:51:30
Sc3M

Macroporous Cement

Pénétration de Graftys® HBS dans les trabécules

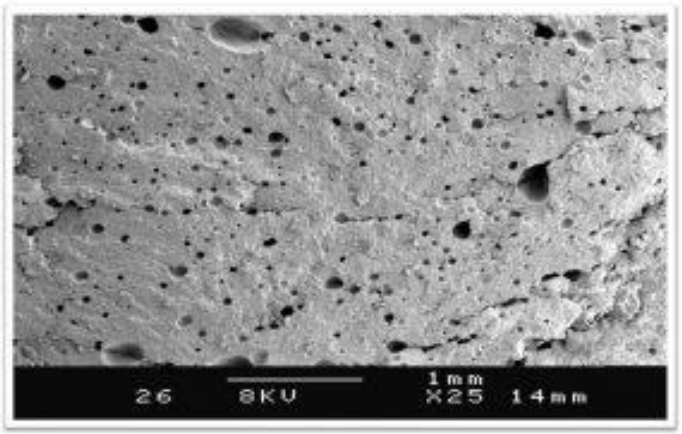

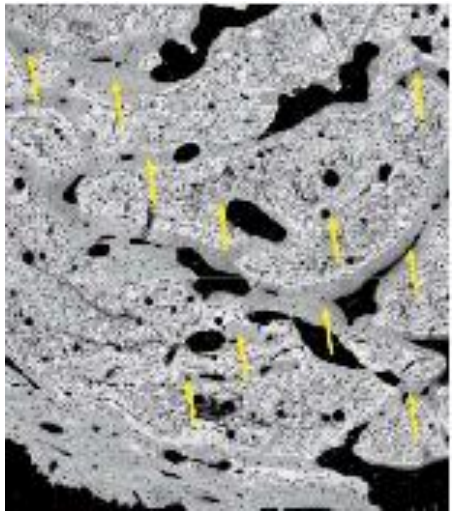

WO 20081023254 A1, 2008, Macroporous and highly resorbable apatitic calcrtm-phosphate cement,
WEISS P, KHAIROUN I, BOULER JM

Mixture of a powder :

- 78 wt %α -tricalcium phosphate (α-TCP),
- 5 wt % dicalcium phosphate dihydrate (CaHPO4,2H2 O)
- 5 wt % monocalcium phosphate mono-hydrate (MCPM)
- 10 wt % calcium-deficient hydroxyapatite (CDA)
- **2 wt % HPMC**.

liquid phase : 5 wt % Na2HPO4 aqueous solution

Graftys® QuickSet

About Graftys® QuickSet

Graftys® QuickSet is a Calcium Phosphate Cement of high viscosity with mechanical properties similar to those of cancellous bone, supplied in a user-friendly double-syringe, which is pre-filled with a powder (calcium phosphate salts and HydroxyPropylMethylCellulose (HMPC)) and with a phosphate-based (Na_2HPO_4) aqueous solution. Mixing of these two components in the syringe results in an injectable paste, which hardens under *invivo* The final product formed during the setting reaction is a calcium-deficient apatite CDA that closely mimics the mineral phase of natural bone.

Total porosity measured by Hg intrusion (%)

61 ± 6 / 44± 4

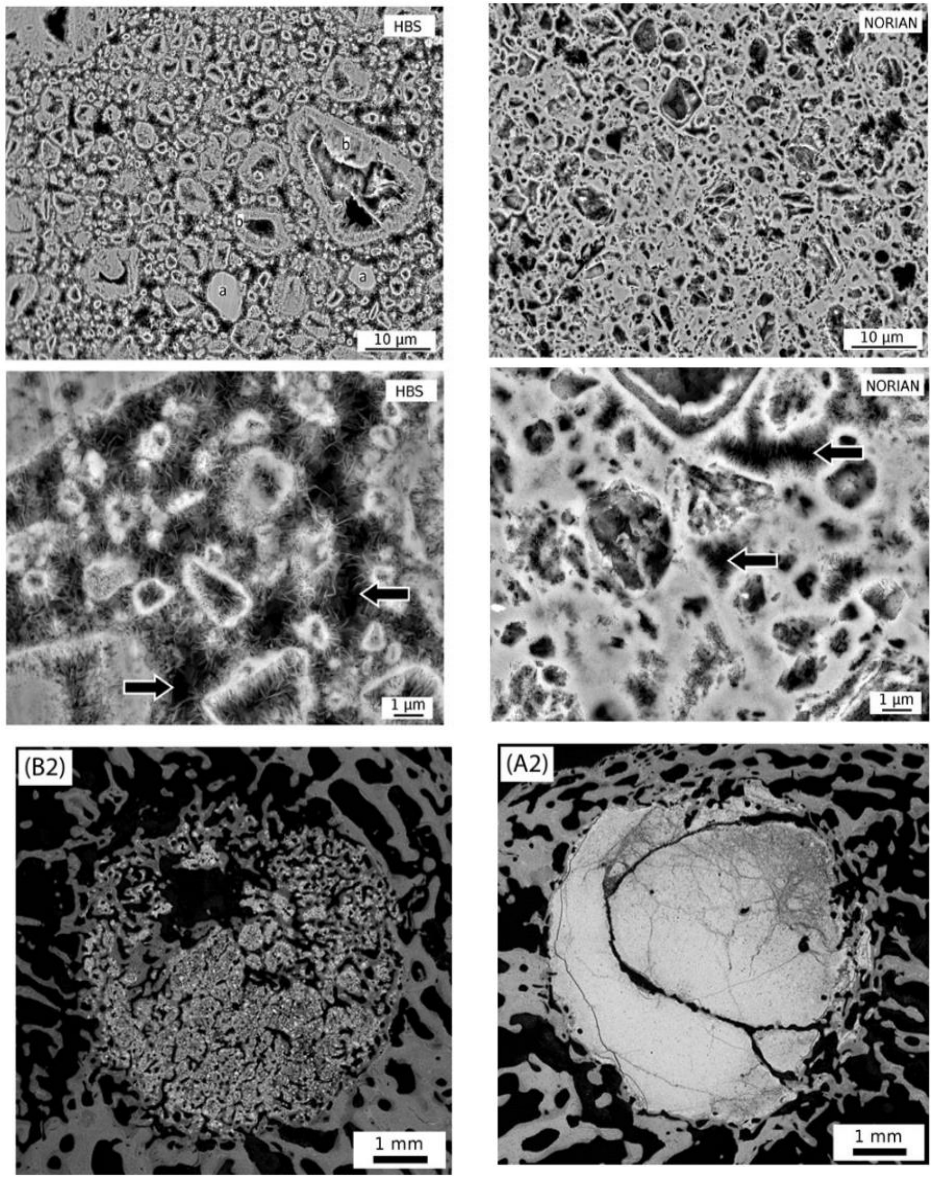

ORIGINAL RESEARCH REPORT

WILEY

In vivo resorption of injectable apatitic calcium phosphate cements: Critical role of the intergranular microstructure

Myriam Le Ferrec[1,2] | Charlotte Mellier[1] | Francois-Xavier Lefèvre[3] | Florian Boukhechba[1] | Pascal Janvier[3] | Gilles Montavon[2] | Jean-Michel Bouler[3] | Olivier Gauthier[4,5] | Bruno Bujoli[3]

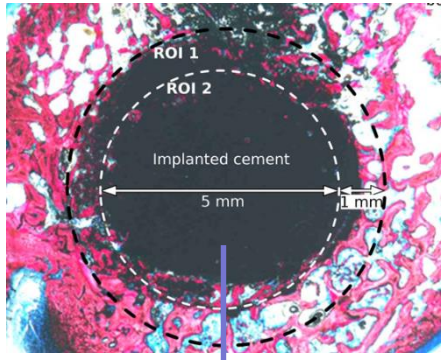

Implantation time	HBS		NORIAN	
	Cement area density (%)	Bone area density (%)	Cement area density (%)	Bone area density (%)
4 weeks	88.6 ± 13.2	5.6 ± 1.7*	99.0 ± 0.9	0.6 ± 0.2
8 weeks	76.9 ± 15.5*	13.5 ± 4.1*	98.9 ± 0.9	0.8 ± 0.2
12 weeks	79.1 ± 15.7*	11.0 ± 3.3*	97.5 ± 0.9	1.5 ± 0.5

8 weeks of implantation
in Rabbit bone

Commercialized injectable bone subtitutes

Biological properties — Mechanical properties

In'Oss™ MBCP™

Injectable suspensions

MBCP™ Putty - In'Oss™

+ Biocompatibility
+ Injectability
+ Osteoconduction

- Mechanical properties

Hydroxyapatite + Phosphate Tricalcique Bêta (ßTCP)
+ viscous liquid = 2% HPMC

Biomatlante
Biologics Solutions

WO 9521634 (A1) Injectable Bone Substitute : WEISS P, DACULSI G,, DELECRIN J, GRIMANDI G ET PASSUTI N

Solid materials

Graftys® QuickSet

+ Biocompatibility
+ Injectability
+ mechanical properties

- Porosity = HPMC particules
- Osteoconduction

Graftys®

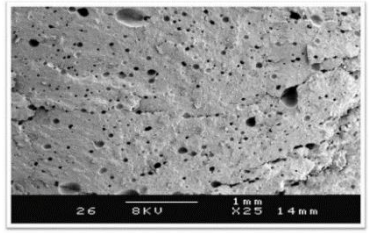

calcium phosphate salts + HydroxyPropylMethylCellulose (HPMC)) + Na_2HPO_4

WO 20081023254 A1, 2008, Macroporous and highly resorbable apatitic calcrtm-phosphate cement, WEISS P, KHAIROUN I, BOULER JM

Materials Advances

ROYAL SOCIETY OF CHEMISTRY

REVIEW

View Article Online
View Journal | View Issue

Check for updates

Cite this: *Mater. Adv.*, 2022, 3, 6125

Injectable macromolecule-based calcium phosphate bone substitutes

Hilel Moussi,[ab] Pierre Weiss,[a] Jean Le Bideau,[b] Hélène Gautier[a] and Baptiste Charbonnier[a]

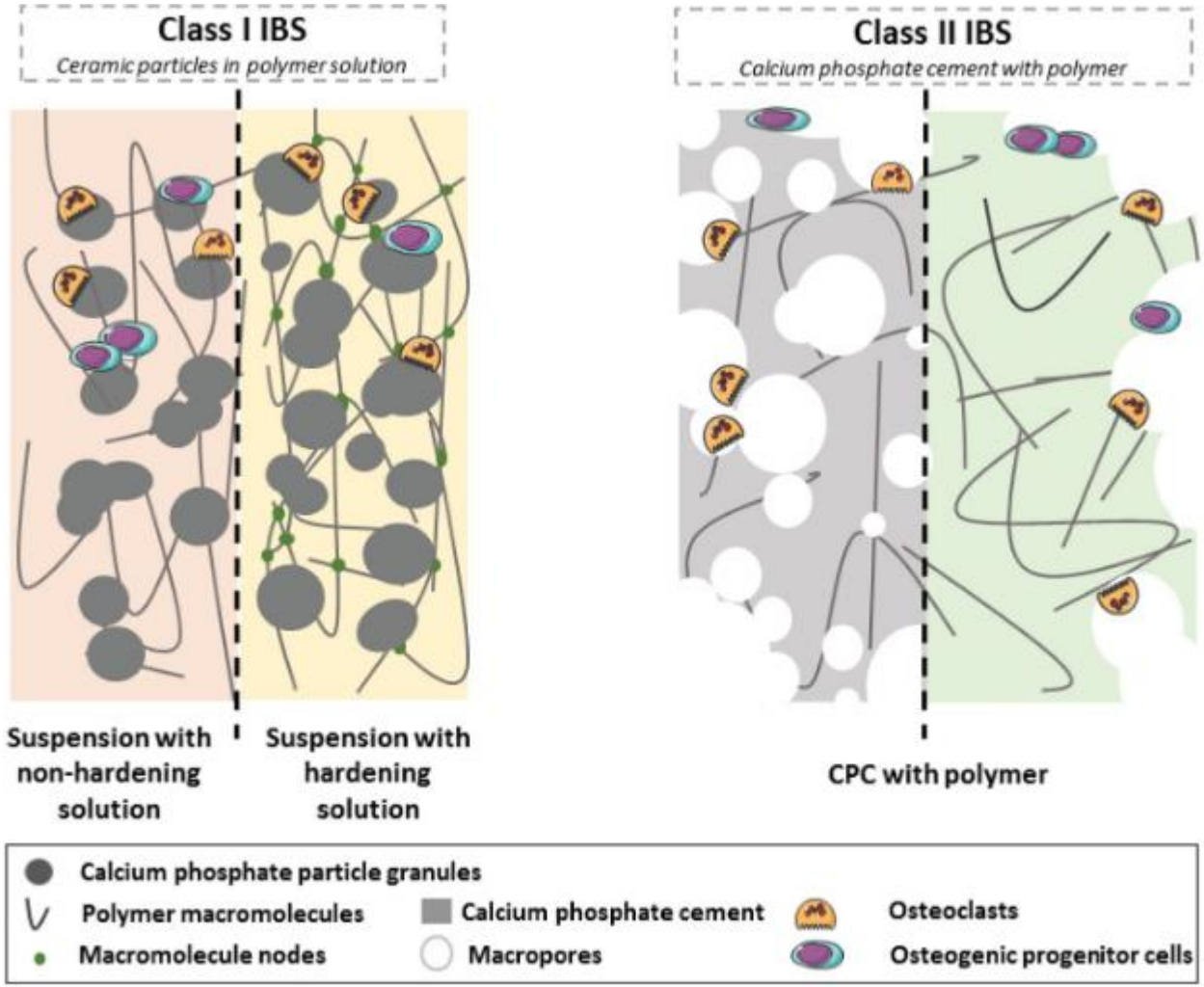

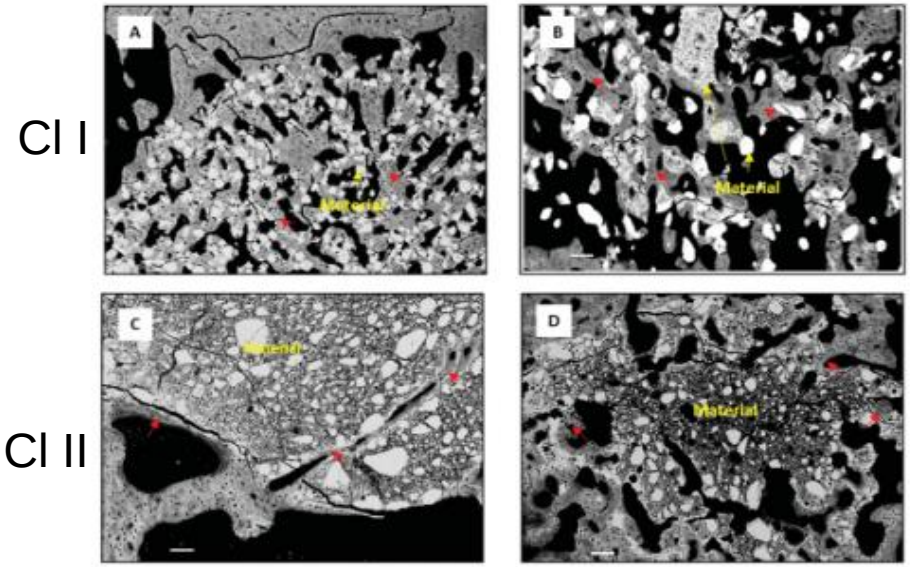

Fig. 1 The two classes of IBS present different osteoconduction mechanisms: for Class I, calcium phosphate supports are made of divided ceramics (thermally-sintered particles, resulting in high density materials); for Class II, calcium phosphate supports are made of bulk cements (soft chemistry route to interlinked particles, resulting in low-density materials showing macropores).

Materials Advances

ROYAL SOCIETY OF CHEMISTRY

REVIEW

View Article Online
View Journal | View Issue

Check for updates

Cite this: *Mater. Adv.*, 2022, 3, 6125

Injectable macromolecule-based calcium phosphate bone substitutes

Hilel Moussi,[ab] Pierre Weiss,[*a] Jean Le Bideau,[b] Hélène Gautier[a] and Baptiste Charbonnier[a]

Table 1 Class I and Class II injectable and extrudable commercialized materials currently on the market (TCP = tricalcium phosphate, HA = hydroxyapatite, CaP = calcium phosphate, CDHA = calcium deficient hydroxyapatite, HPMC = hydropropylmethylcellulose, rhBMP = recombinant human bone morphogenetic protein)

Commercial name and manufacturer	Material class	Inorganic phase	Organic phase	Application	Characteristics	Clinical trial number and reference
MBCP-Gel/In'Oss™ (Biomatlante)	I	CaP granules	HPMC polymer solution	Filling osseous defects of various origins	Ready to use, cohesivity/ putty	NCT00740311; (ref. 30)
ExcelOs-inject (CGBIO)	I	Beta TCP granules	Biodegradable hydrogel with or without rhBMP-2	Spinal fusion	Ready to use, injectable, cohesivity	NCT02714829; (ref. 31)
Mastergraft (Medtronic)	I	β-TCP + HA	Bovine collagen matrix	Spinal fusion	Putty	NCT01491542; (ref. 32)
Vitoss (Stryker)	I	β-TCP granules	Bone marrow aspirate	Spinal pathologies	Putty ultra-porous, flexible	NCT03509480; (ref. 33)
ChronOS (DePuy Synthes)	I	β-TCP granules	Autologous blood and/or bone marrow	Tibial plateau fractures	Putty	NCT02056834; (ref. 34)
ChronOS Inject (DePuy Synthes)	I	Brushite matrix and (TCP) granules		Proximal tibial fractures	Injectable, degradable	NCT02056834; (ref. 35)
CERAMENT® (Bone Void Filler)	I	HA and calcium sulfate cement		Tibial plateau fractures	Injectable, degradable	NCT01828905; (ref. 36)
Norian® Drillable (DePuy Synthes)	II	Carbonated apatite cement	Bioresorbable polylactide/ glycolide copolymer fibres	Tibial fractures	Mechanical resistance 24 hours after injection	NCT01132508; (ref. 37)
Graftys quickset/ HBS (Graftys)	II	CDHA cement	Powder of HPMC polymer	Bone disease, bone fractures	Porosity	NCT02575352; (ref. 38)

Materials Advances

ROYAL SOCIETY OF CHEMISTRY

REVIEW

View Article Online
View Journal | View Issue

Check for updates

Cite this: *Mater. Adv.*, 2022, 3, 6125

Injectable macromolecule-based calcium phosphate bone substitutes

Hilel Moussi,[ab] Pierre Weiss,[ab]* Jean Le Bideau,[b] Hélène Gautier[a] and Baptiste Charbonnier[a]

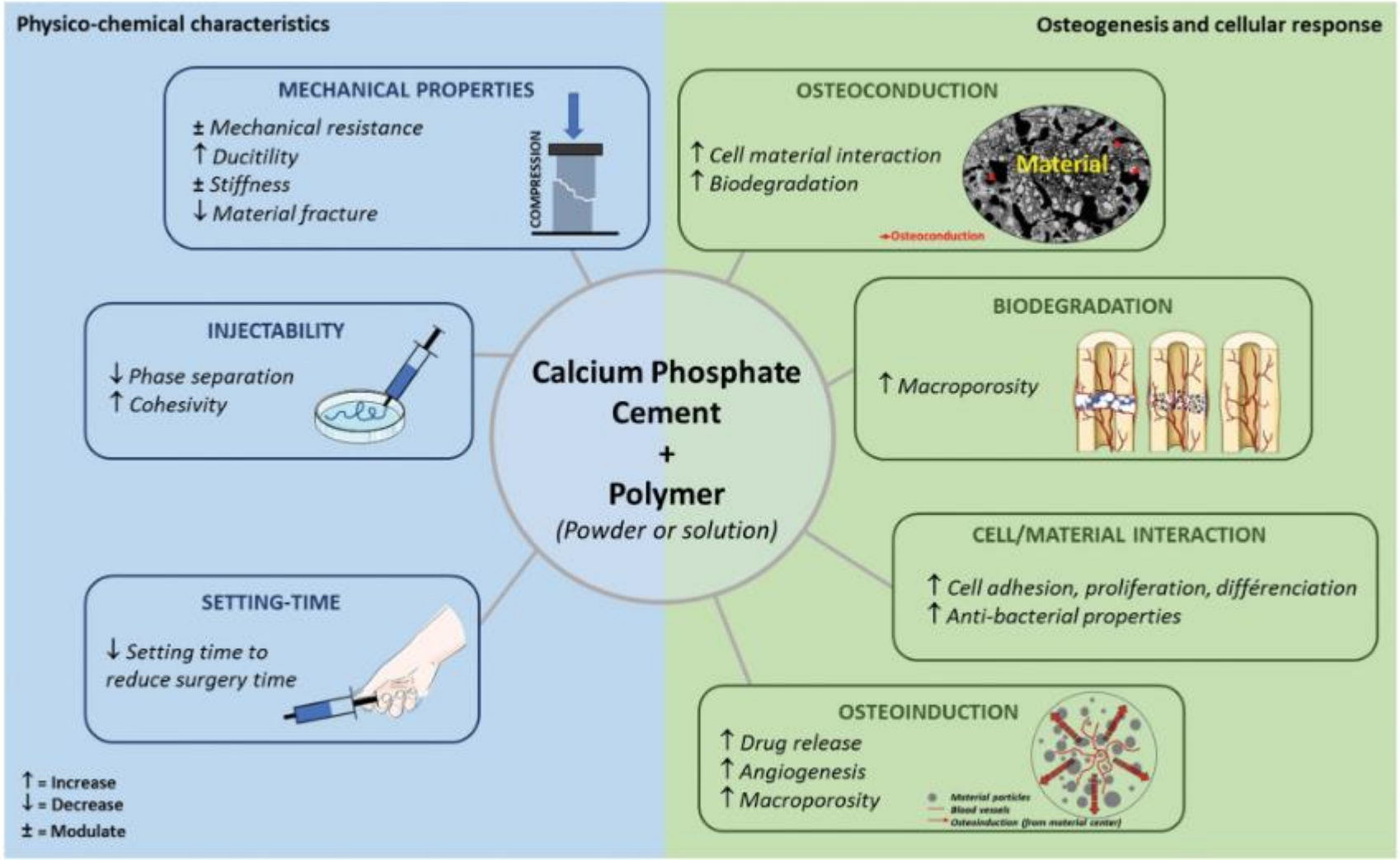

Modulation of IBS properties by a combination of polymers with calcium phosphate cement (Class II).

Physico-chemical characterization

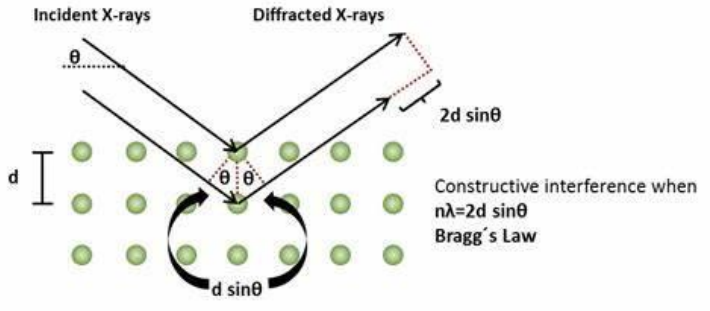

X-ray diffraction

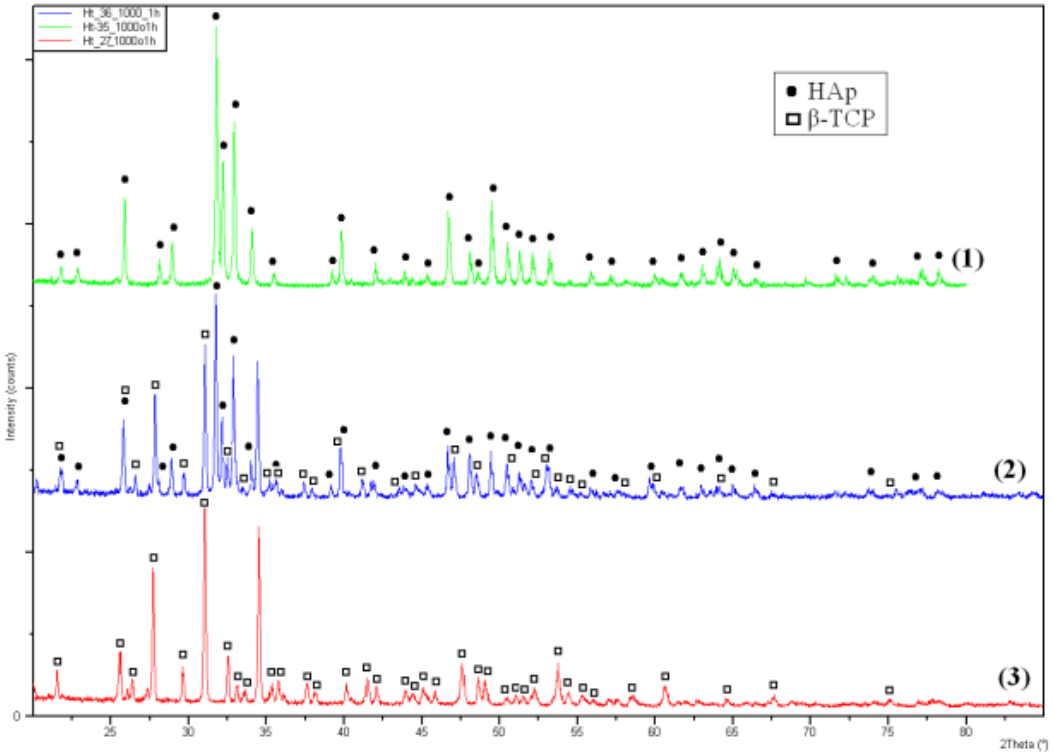

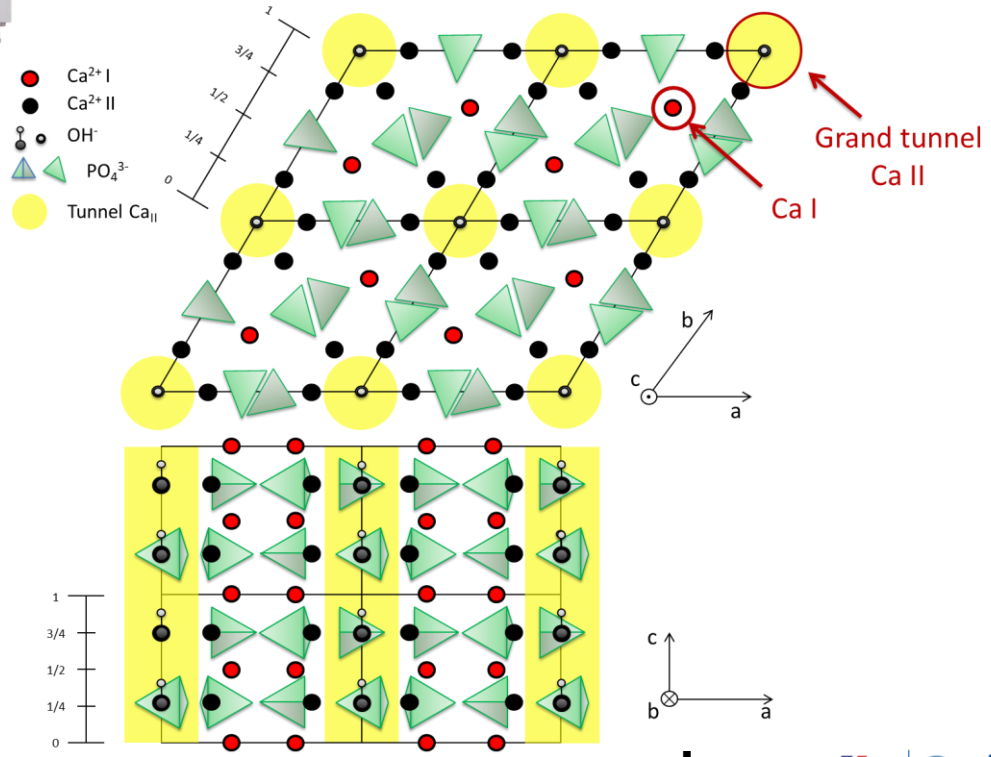

Physico-chemical characterization

Infrared Spectroscopie

$Ca_{10-x}(PO_4)_{6-x}(CO_3)_x(OH)_{2-x-2y}(CO_3)_y$

Bandes IR (cm-1)	Intensité	Attribution	
3700 - 3000	moyenne	H-O-H, H2O adsorbée	
3640 et 3540	faible	O-H, des groupes Ca(OH)2	
3580	épaulement	O-H, vibration de valence symétrique des ions OH^-	ν_S
1630	moyenne	H2O et CO2 adsorbés	
1400 – 1380 *	forte	N-O des groupes NO3	
1500 - 1350	faible	C-O des groupes CO3	ν_3
1200 - 1180	épaulement	P-OH, groupes HPO4	
1120 - 1020	forte	P-O, élongation antisymétrique des ions $PO4^{3-}$	ν_3
965 - 960	moyenne	P-O, élongation symétrique des ions $PO4^{3--}$	ν_1
900 - 850	faible	C-O des groupes CO3	ν_2
880 - 865	faible	Elongation P-OH des groupes HPO4	
820 *	faible	N-O des groupes NO3	
630	épaulement	O-H mouvement de libration des ions OH^-	ν_L
600 - 550	forte	P-O, déformation antisymétrique des ions $PO4^{3-}$	ν_4
460	faible	P-O, déformation symétrique des ions $PO4^{3-}$	ν_2

*Résidus nitrés de synthèse présents dans une poudre immédiatement après synthèse ; la majorité des nitrates étant éliminés par traitement thermique de la poudre à faible température (T ≈ 400 °C).

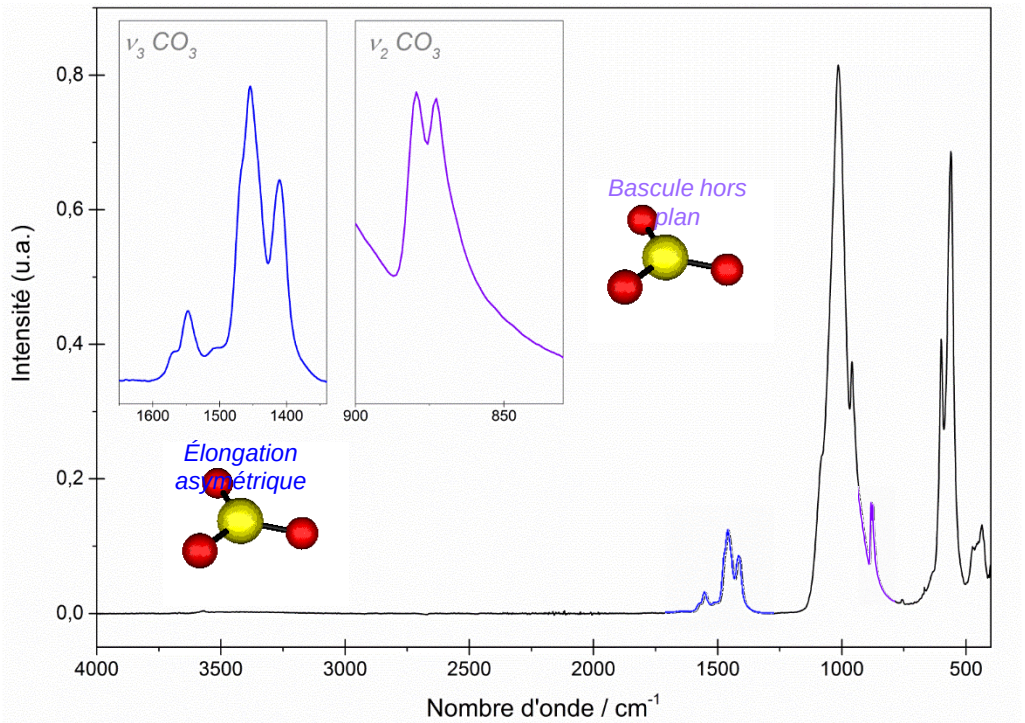

Physico-chemical characterization

Analyses élémentaires

ICP-AES (ICP-MS également possible!)

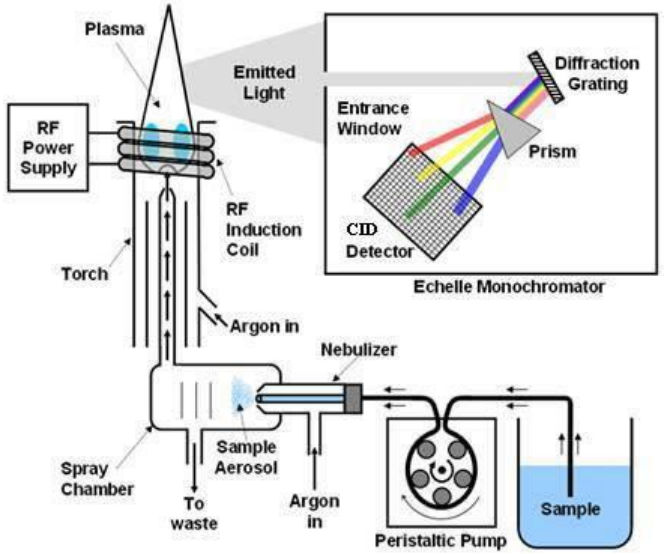

Dosages chimiques (chromato ionique, dosage C,…)

Physico-chemical characterization

Microscopie électronique à balayage

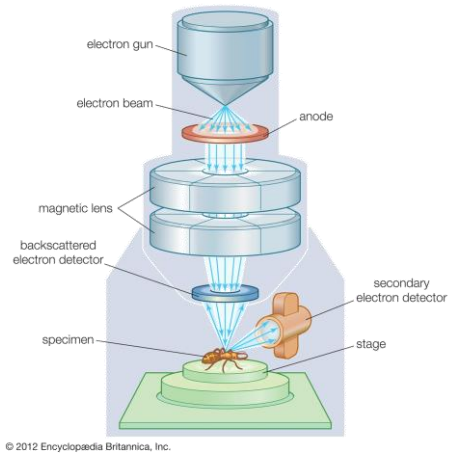

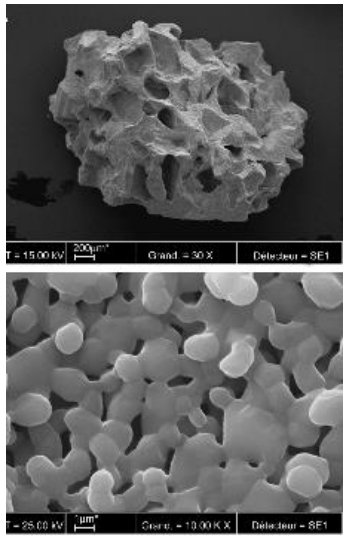

Microscopie électronique en transmission

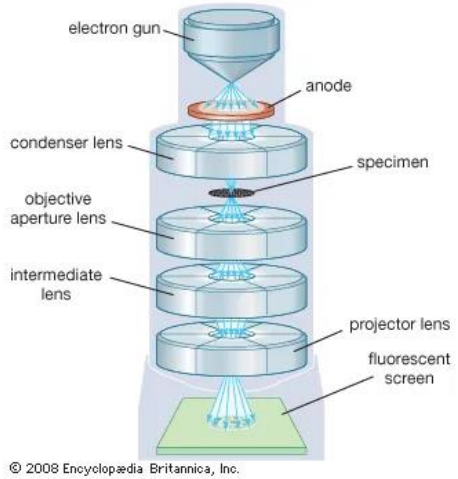

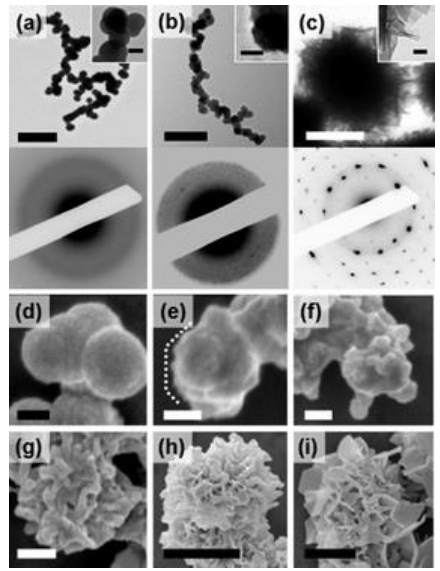

Pan et al., Mystery of the transformation from amorphous calcium phosphate to hydroxyapatite, Chem. Comm. (2010)

Physico-chemical characterization

Micro/Nano tomographie à rayons X

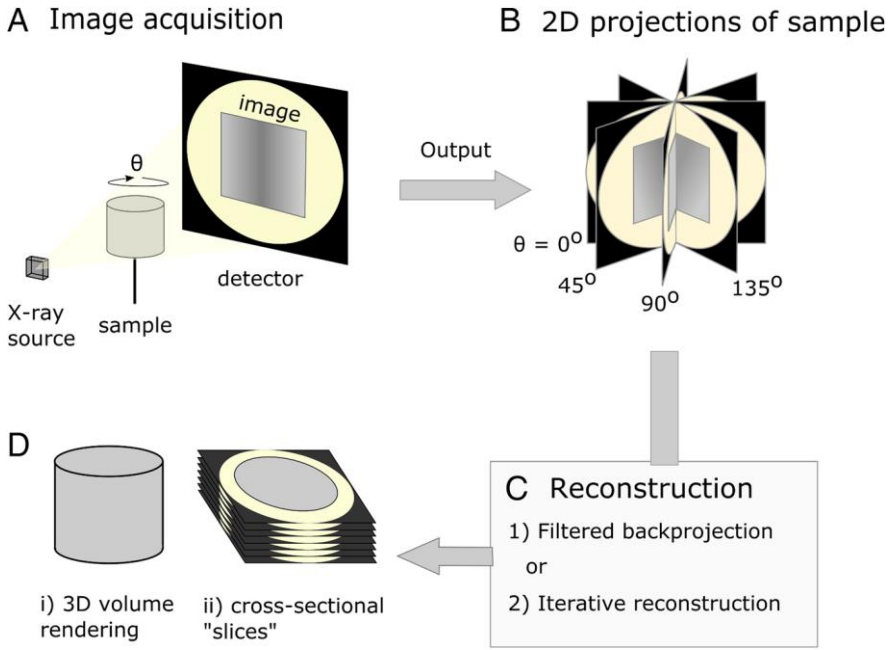

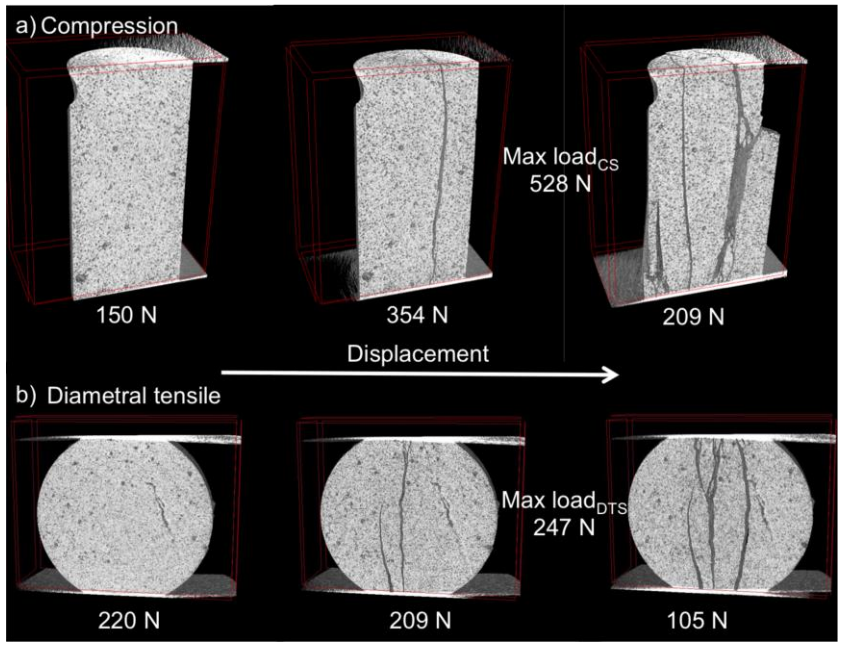

Physico-chemical characterization

Essais Mécaniques

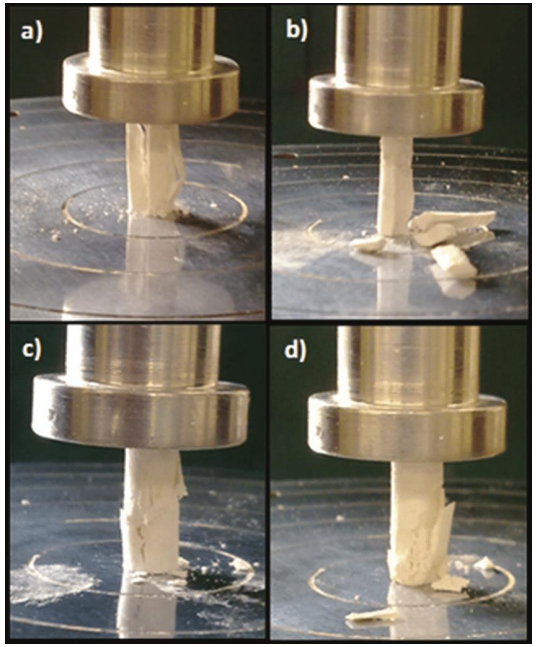

Property	**Cortical bone**	Calcium phosphate cement
Specific Gravity (g/cm3)	1,7-2,1	1,7-2,0
Tensile Strength (MPa)	60-160	2,1-14
Compressive strength (MPa)	13-18	20-91
Young's Modulus (GPa)	3-30	35-105
Fracture energy (J/m2)	390-560	–
Resistance to fracture (Mpa/m2)	2-12	0,3-0,8
Composition	Inorganic + organic	Inorganic

Source: Adapted from Wagh (2016)

Physico-chemical characterization

Injectabilité et temps de prise (ciment)

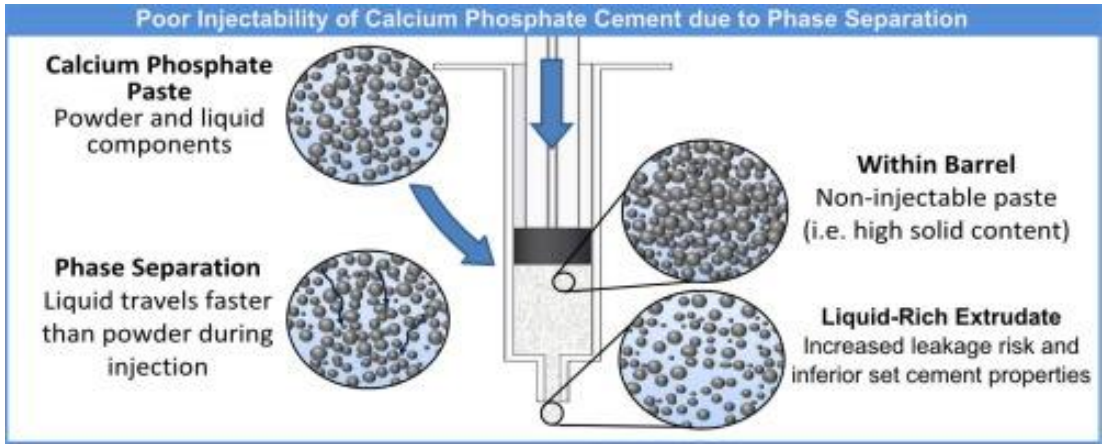

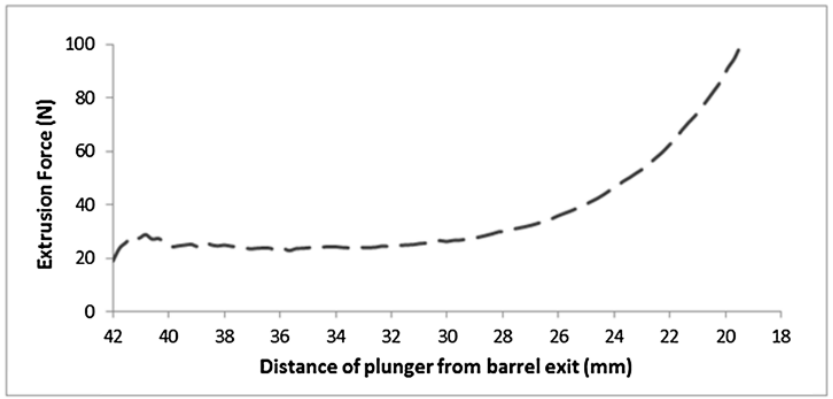

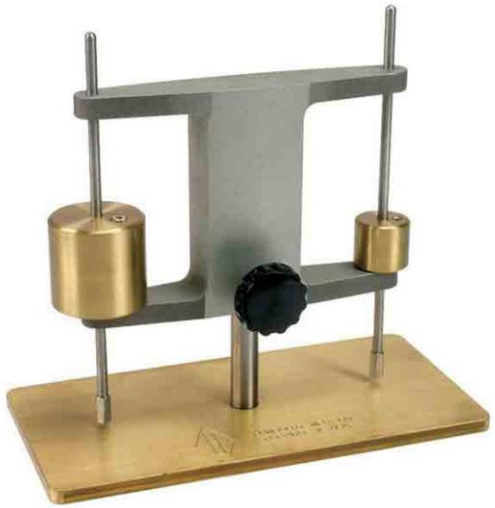

Physico-chemical characterization

Comportement rhéologique (ciment)

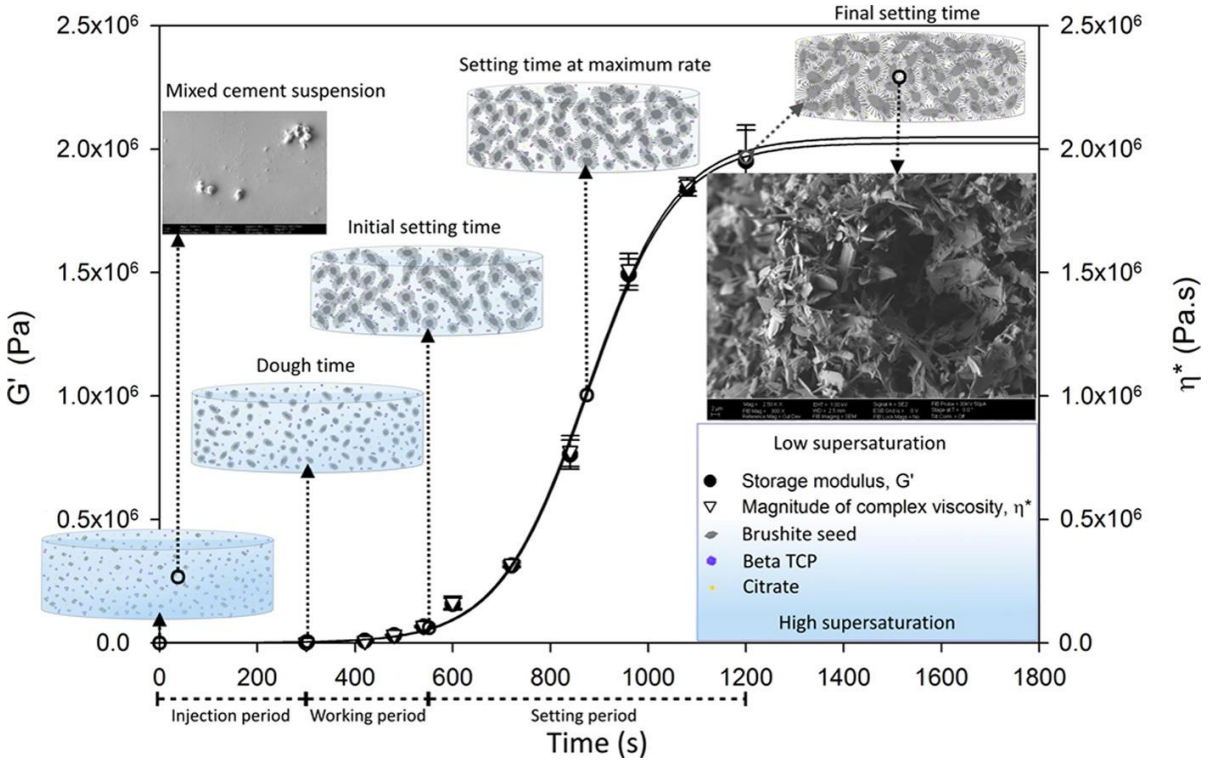

Erdem et al., The rheological behavior of a fast-setting calcium phosphate bone cement and its dependence on deformation conditions (2017)

Physico-chemical characterization

Comportement en milieu biologique simulé

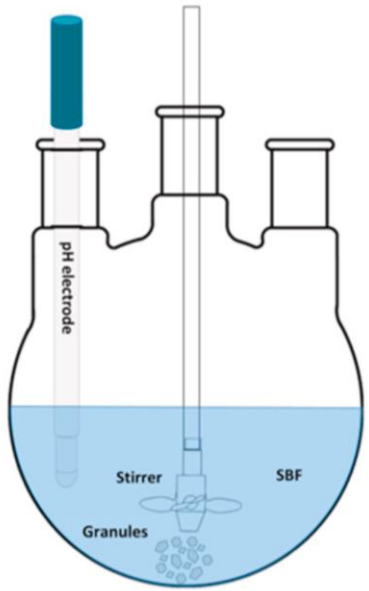

Mazzoud et al., Cell-free, quantitative mineralization measurements as a proxy to identify osteoinductive bone graft substitutes, Biomaterials 2022

Analyses multimodales

Changement:

- Composition
- Phases
- Masse
- Porosité
- Surface spécifique
- Morphologie…

Scaffold for cells = osteoconduction

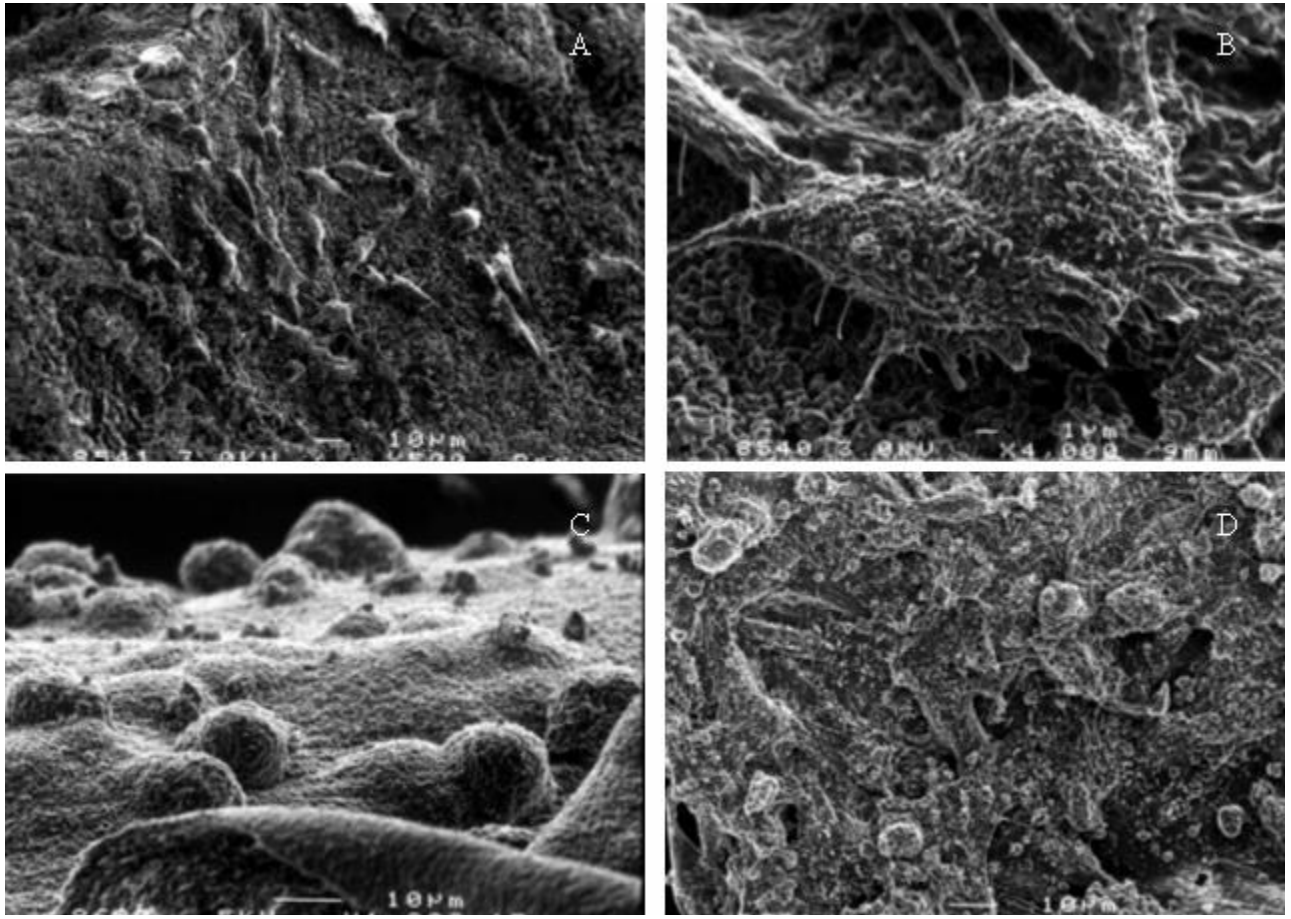

Osteoconduction

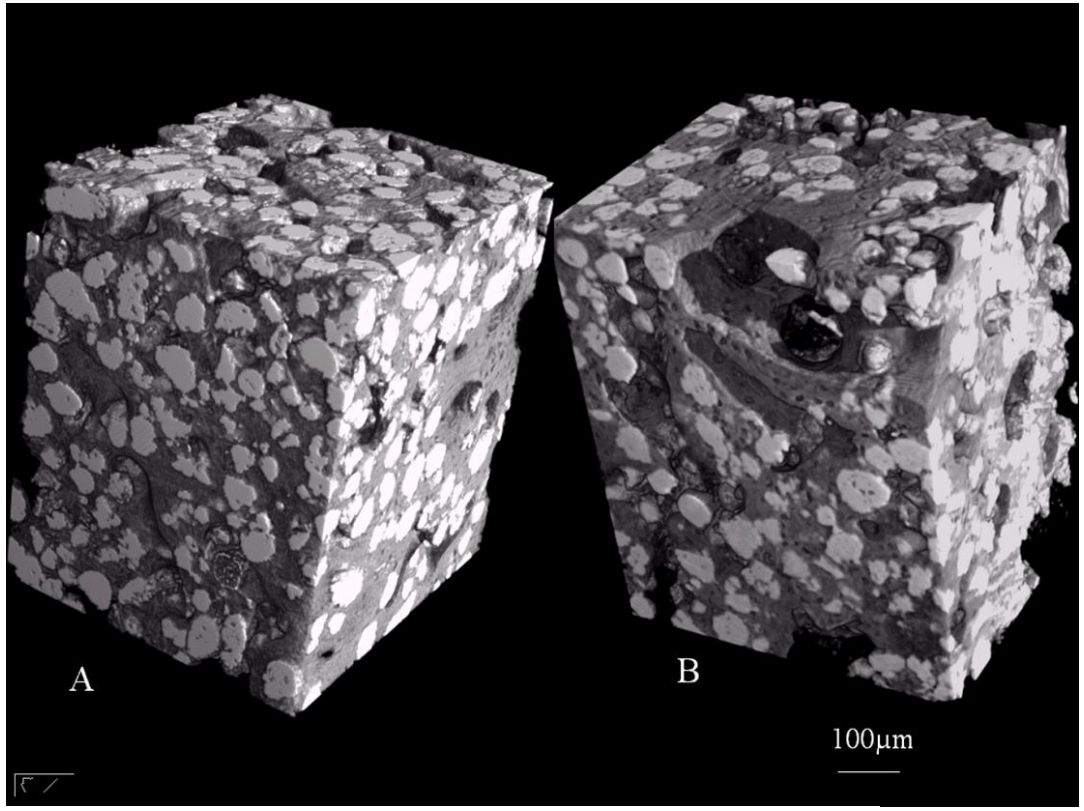

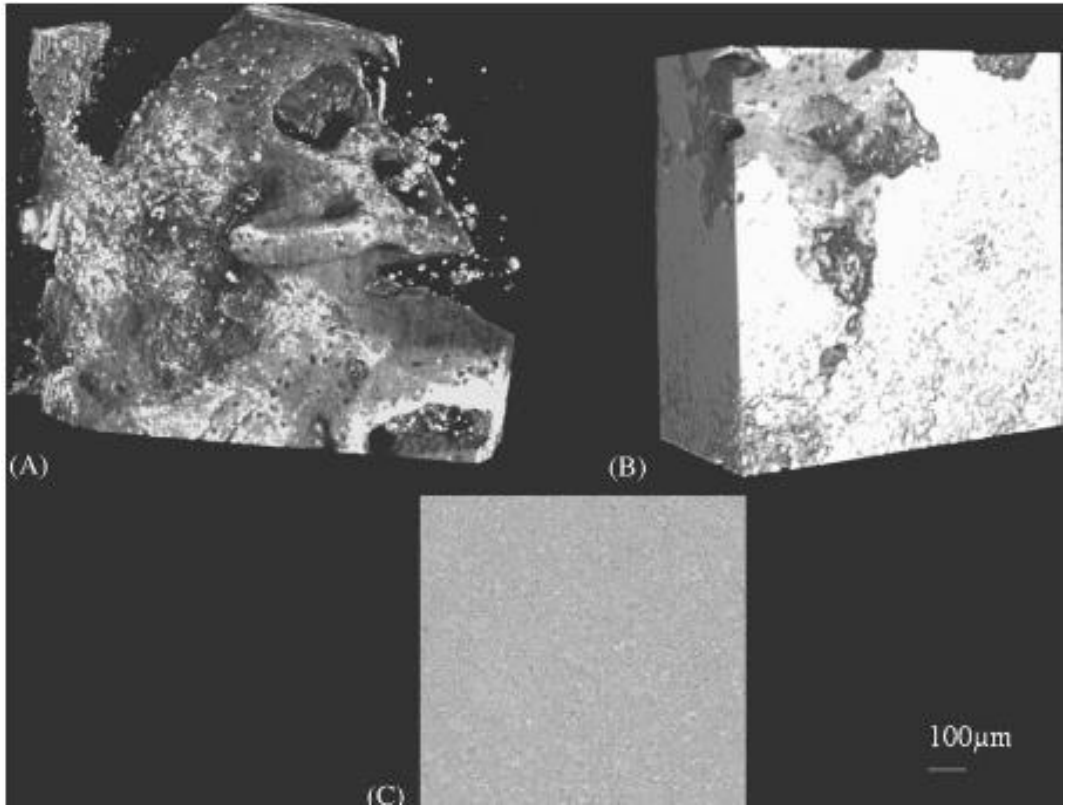

ELSEVIER

Available online at www.sciencedirect.com
SCIENCE DIRECT®

Biomaterials 24 (2003) 4591–4601

Biomaterials

www.elsevier.com/locate/biomaterials

Synchrotron X-ray microtomography (on a micron scale) provides three-dimensional imaging representation of bone ingrowth in calcium phosphate biomaterials

P. Weiss[a,*], L. Obadia[a], D. Magne[a], X. Bourges[a], C. Rau[b], T. Weitkamp[b], I. Khairoun[a], J.M. Bouler[a], D. Chappard[c], O. Gauthier[a,d], G. Daculsi[a]

Osteoinduction of CaP

Table 1 Histomorphometry of bone formed in porous hydroxyapatite specimens

Animal model	% bone volume
Rabbit	0.5 ± 0.3 (16)
Dog	0.75 ± 0.49 (8)
Baboon	11.3 ± 3.02 (16)

Bone volume was calculated using a Zeiss Integration Platte II with 100 lattice points superimposed over the centre of the sections, as described in Materials and Methods. The number of specimens per animal species is given in parentheses. Values (in %) are means ± s.e.m.

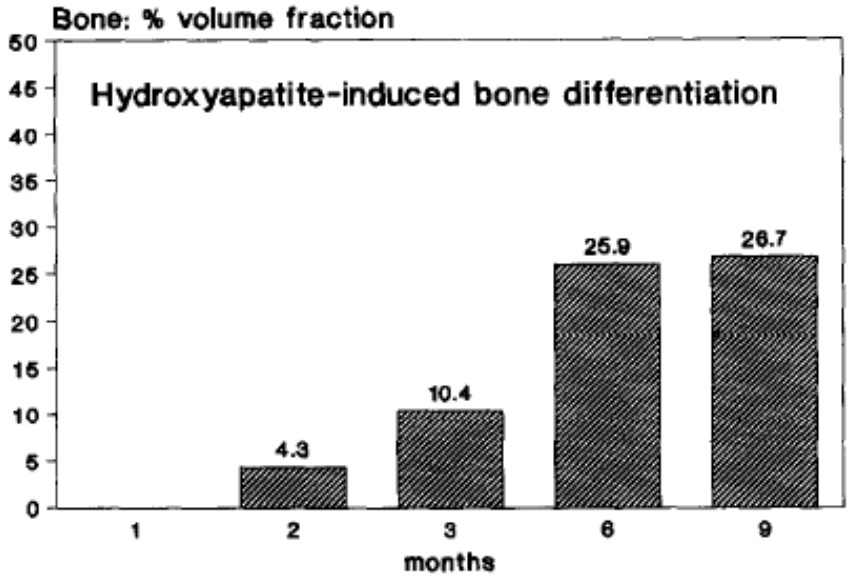

Figure 3 Osteoinduction in coral-derived porous hydroxyapatite after intramuscular implantation in baboons and harvesting at 1, 2, 3, 6 and 9 months. Cumulative means (in %) of histomorphometrical data from Refs 6–9.

Biomaterials 17 (1996) 31–35

0142-9612/96/$15.00

Osteoinduction in porous hydroxyapatite implanted in heterotopic sites of different animal models

Ugo Ripamonti
Medical Research Council/University of the Witwatersrand, Bone Research Laboratory, Medical School, 7 York Road, Parktown, 2193 Johannesburg, South Africa

Frittage

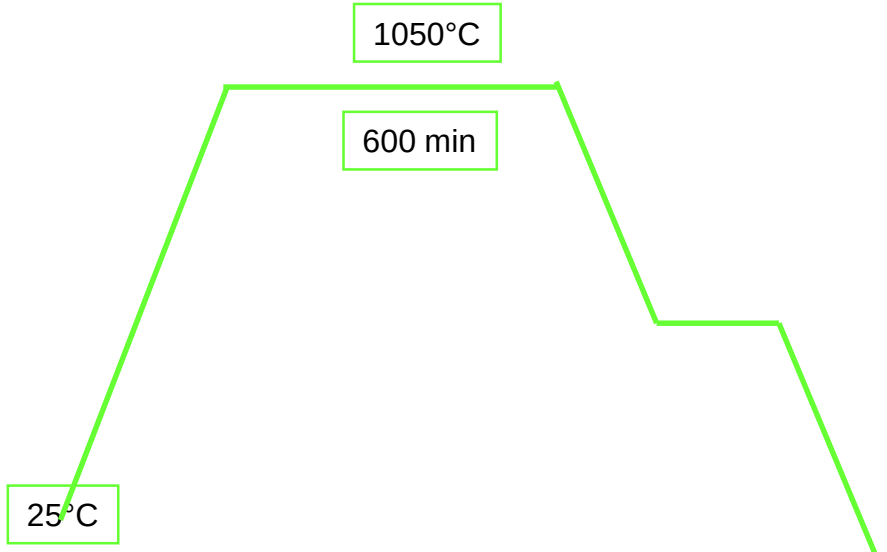

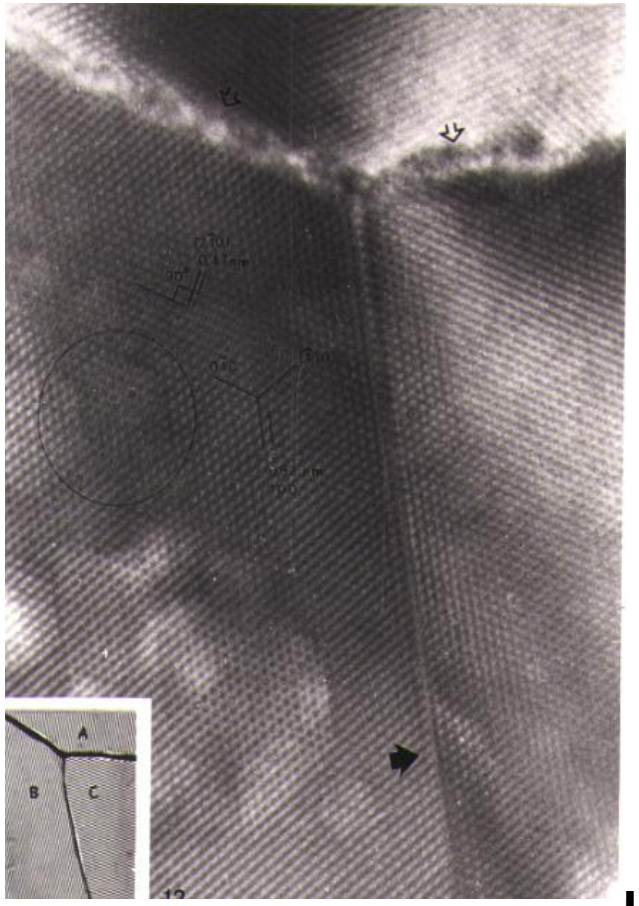

Microstructure et bioactivité

Animal model:

2 goats for 6 weeks

7 goats for 12 weeks

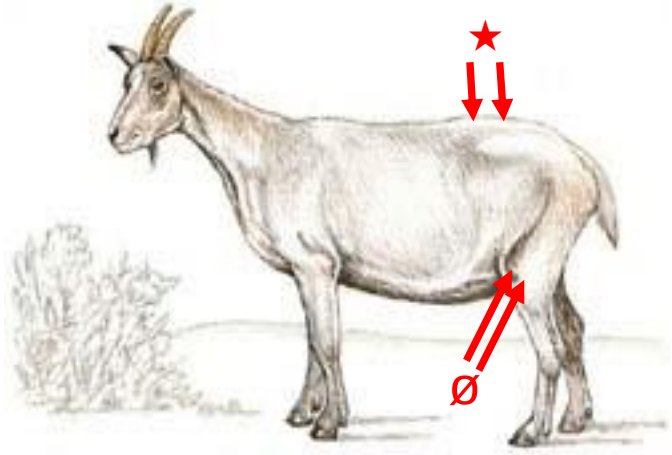

Implant:

Teflon cylinder

2 mm thick walls

(Femoral site)

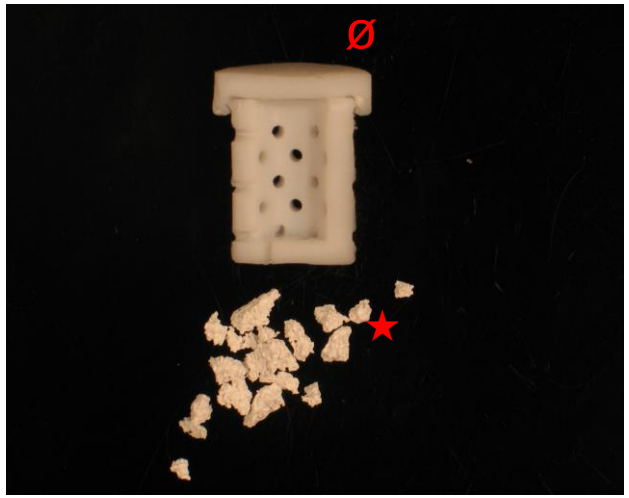

BCP Granules 1-2 mm

1050°C, 1125°C, 1200°C

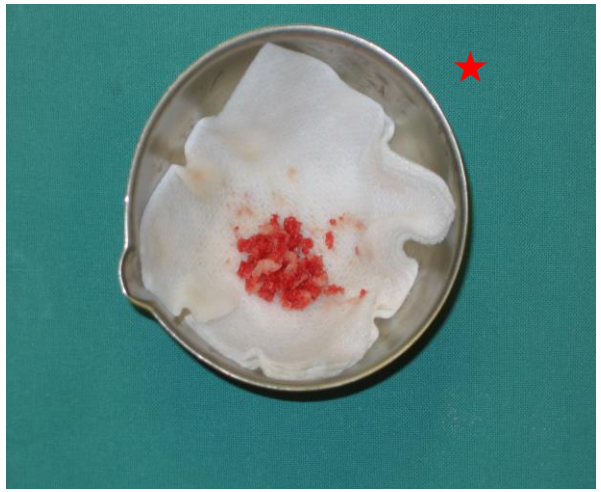

autologous bone chips

BCP ceramics micro porosity

3 sintering Methods

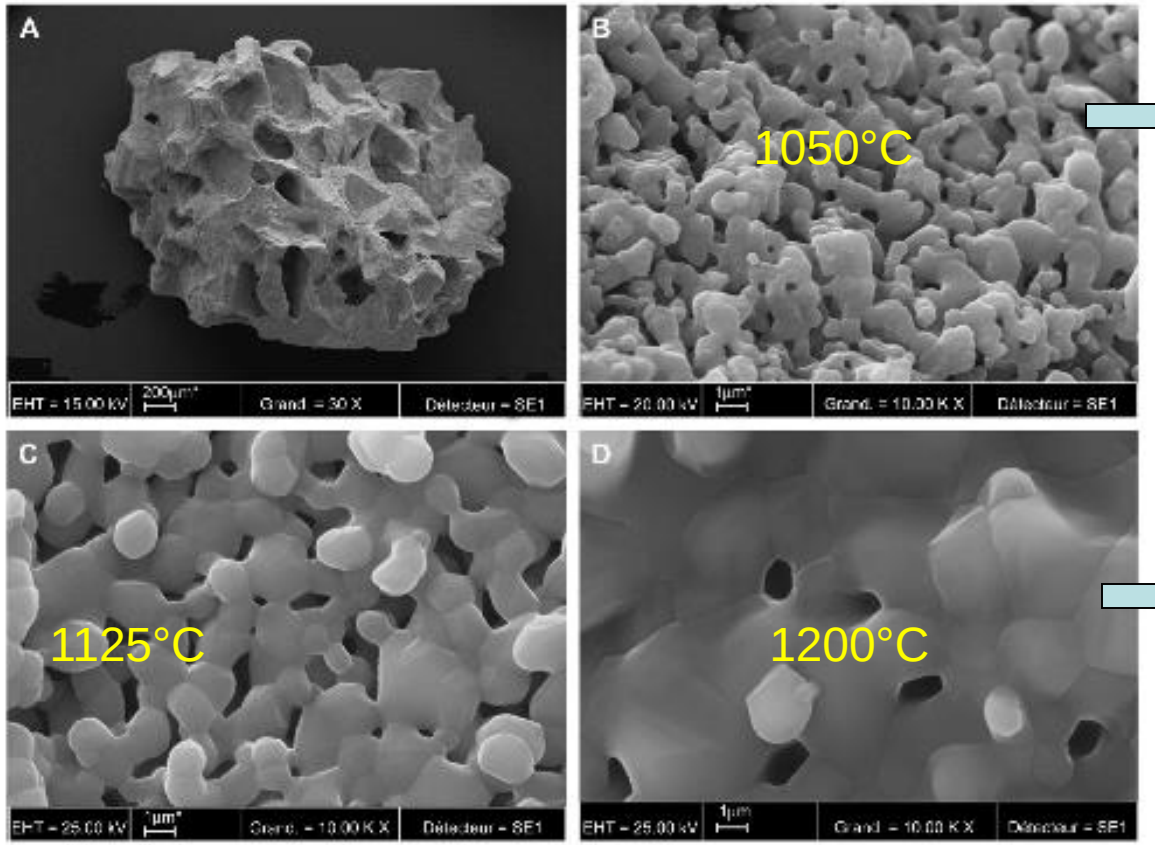

→ Implantation biomaterial

→ Scafold for TE

Fig. 1. SEM micrographs of the BCP granules sintered at different temperatures. (A) General shape of a BCP granule. (B)–(D) High magnification images showing the microstructure of BCP granules sintered at 1050, 1125 and 1200 °C, respectively.

ELSEVIER

Available online at www.sciencedirect.com
ScienceDirect
Biomaterials 29 (2008) 1177–1188

Biomaterials
www.elsevier.com/locate/biomaterials

Osteogenicity of biphasic calcium phosphate ceramics and bone autograft in a goat model

Borhane H. Fellah [a], Olivier Gauthier [b], Pierre Weiss [a], Daniel Chappard [c], Pierre Layrolle [a,*]

Results : Microstructure

Empty cylinder

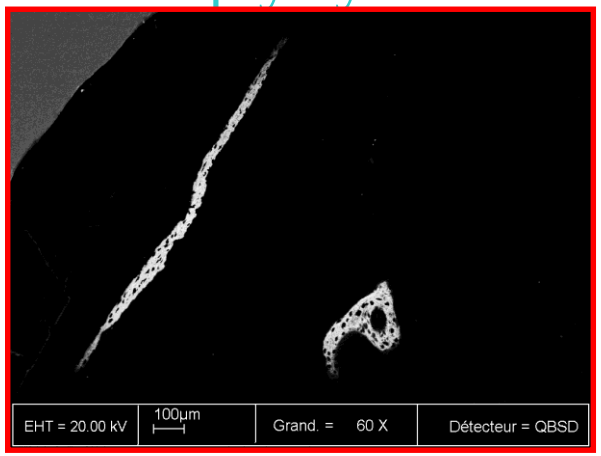

Autologous bone

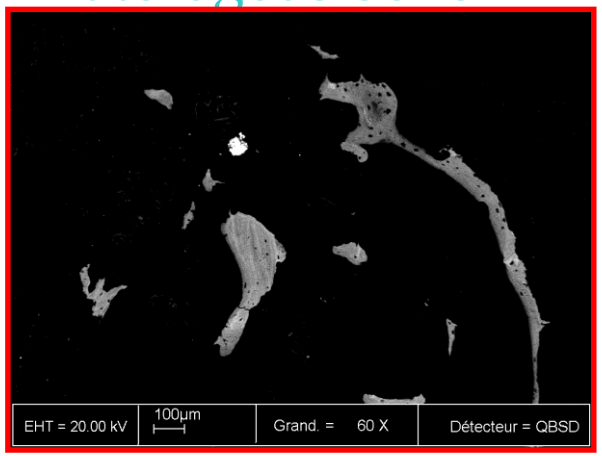

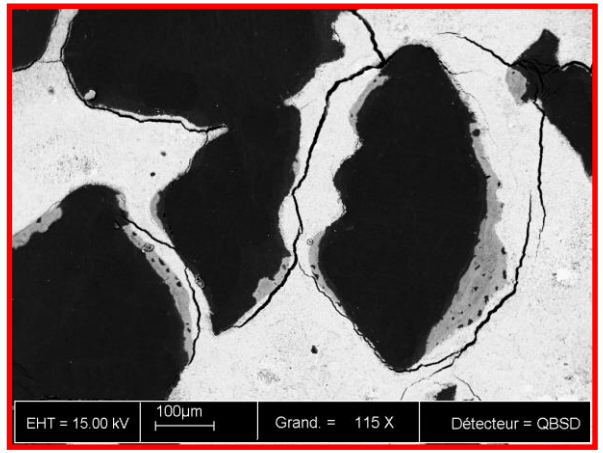

BCP 1050°C

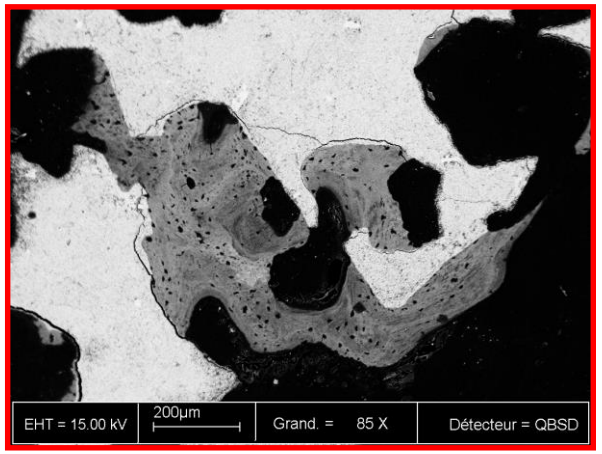

BCP 1125°C

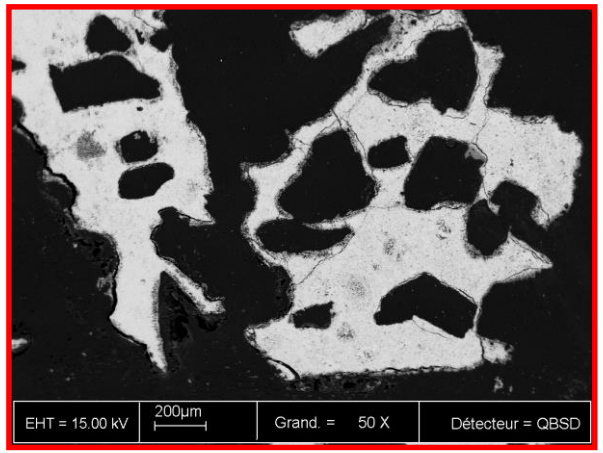

BCP 1200°C

Femurs 12 weeks

Osteoinduction

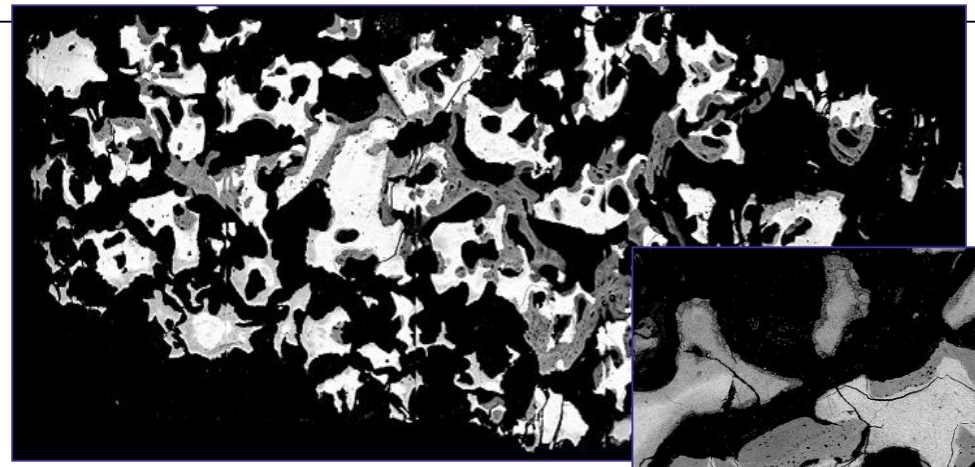

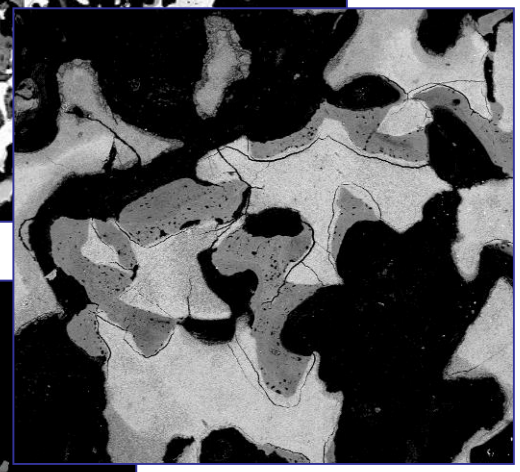

Muscular area

Granules MBCP 1-2mm

6 months in goat

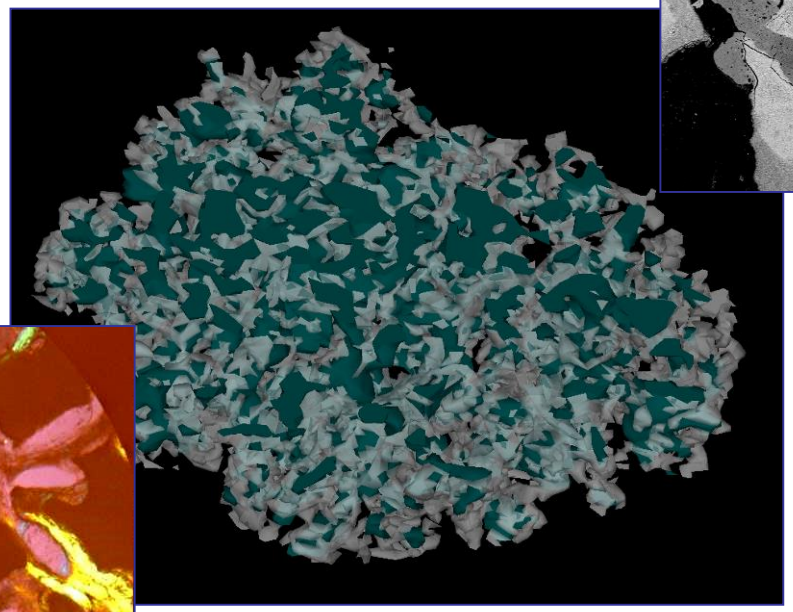

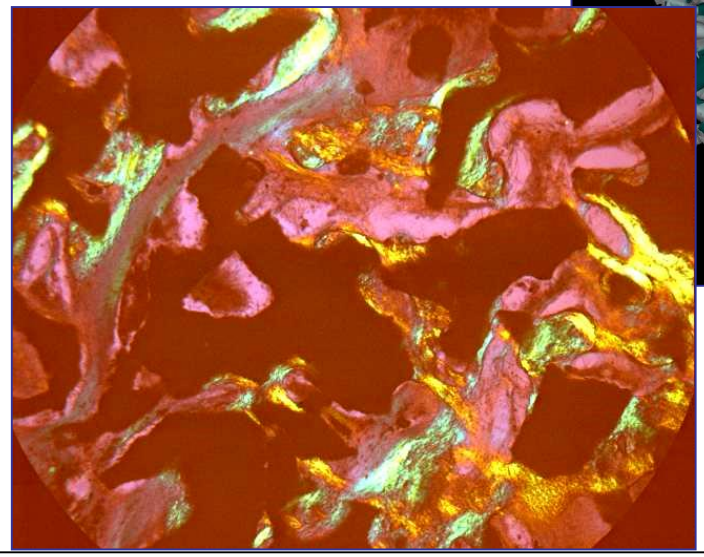

Micropores effect

Calcif.Tiss.Res. 1990

Bone 2005

Biofabrication : Additive manufacturing

Additive Manufacturing

- ‘’Bottom-up’’ procedure

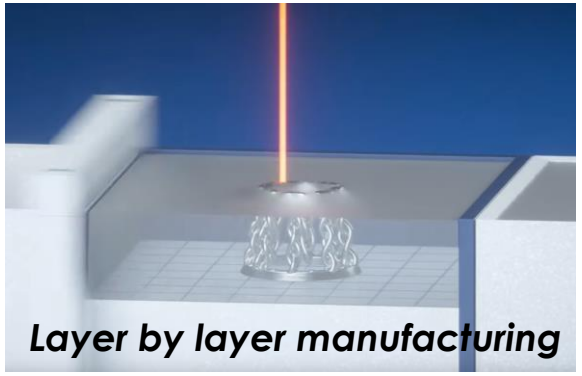

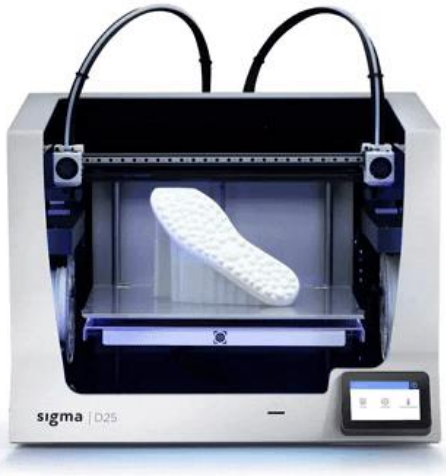

Additive Manufacturing Technologies

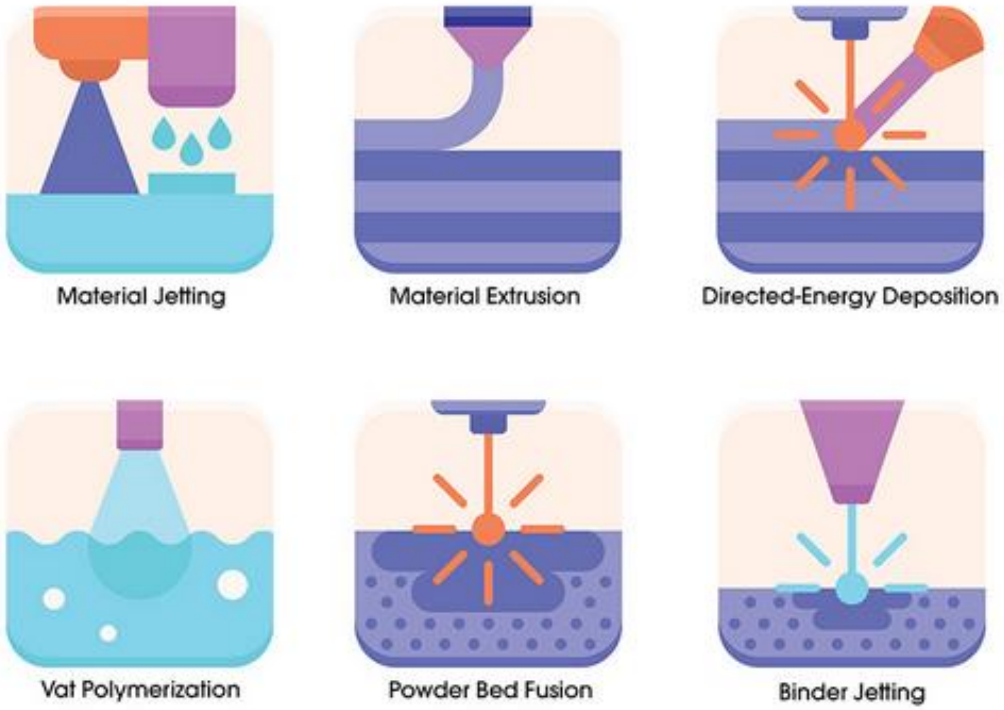

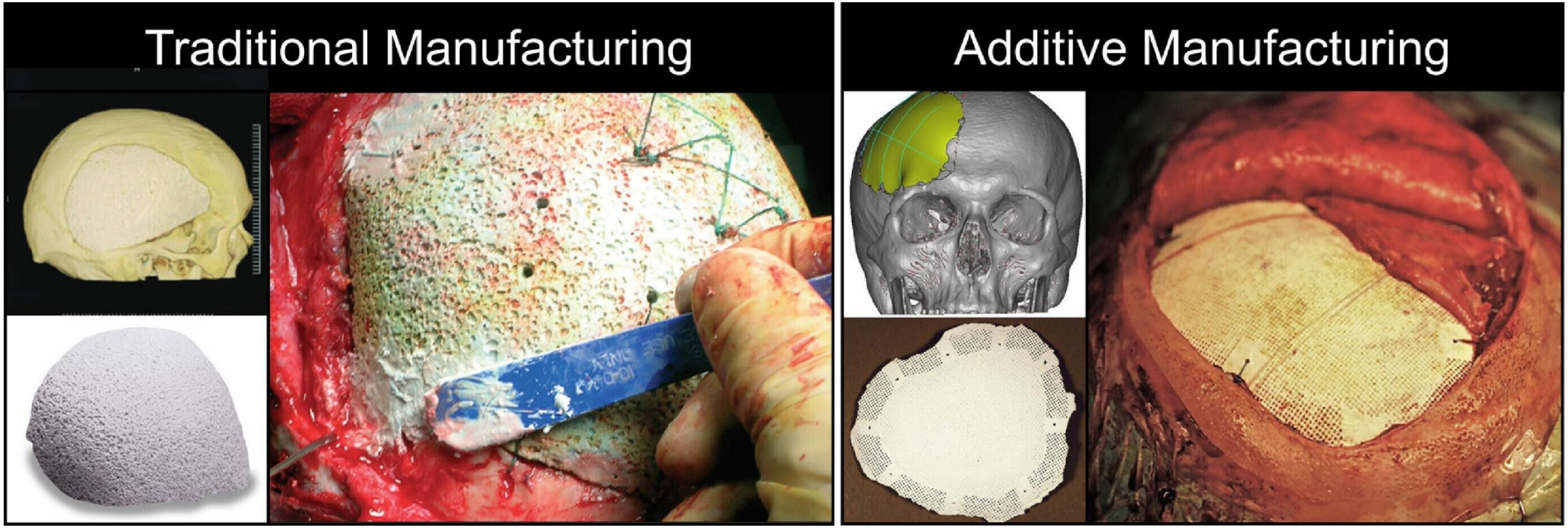

Acta Biomaterialia 121 (2021) 1–28

Contents lists available at ScienceDirect

Acta Biomaterialia

journal homepage: www.elsevier.com/locate/actbio

Review article

Additive manufacturing pertaining to bone: Hopes, reality and future challenges for clinical applications

Baptiste Charbonnier*, Mikhael Hadida, David Marchat

Mines Saint-Etienne, Université de Lyon, Université Jean Monnet, INSERM, U 1059 Sainbiose, 158, cours Fauriel, CS 62362, 42023 Saint-Étienne Cedex 2, France

Progress in Materials Science 130 (2022) 100963

Contents lists available at ScienceDirect

Progress in Materials Science

journal homepage: www.elsevier.com/locate/pmatsci

Additive manufacturing of biomaterials for bone tissue engineering – A critical review of the state of the art and new concepts

Marie-Michèle Germaini [a], Sofiane Belhabib [b], Sofiane Guessasma [c], Rémi Deterre [b], Pierre Corre [a], Pierre Weiss [a,*]

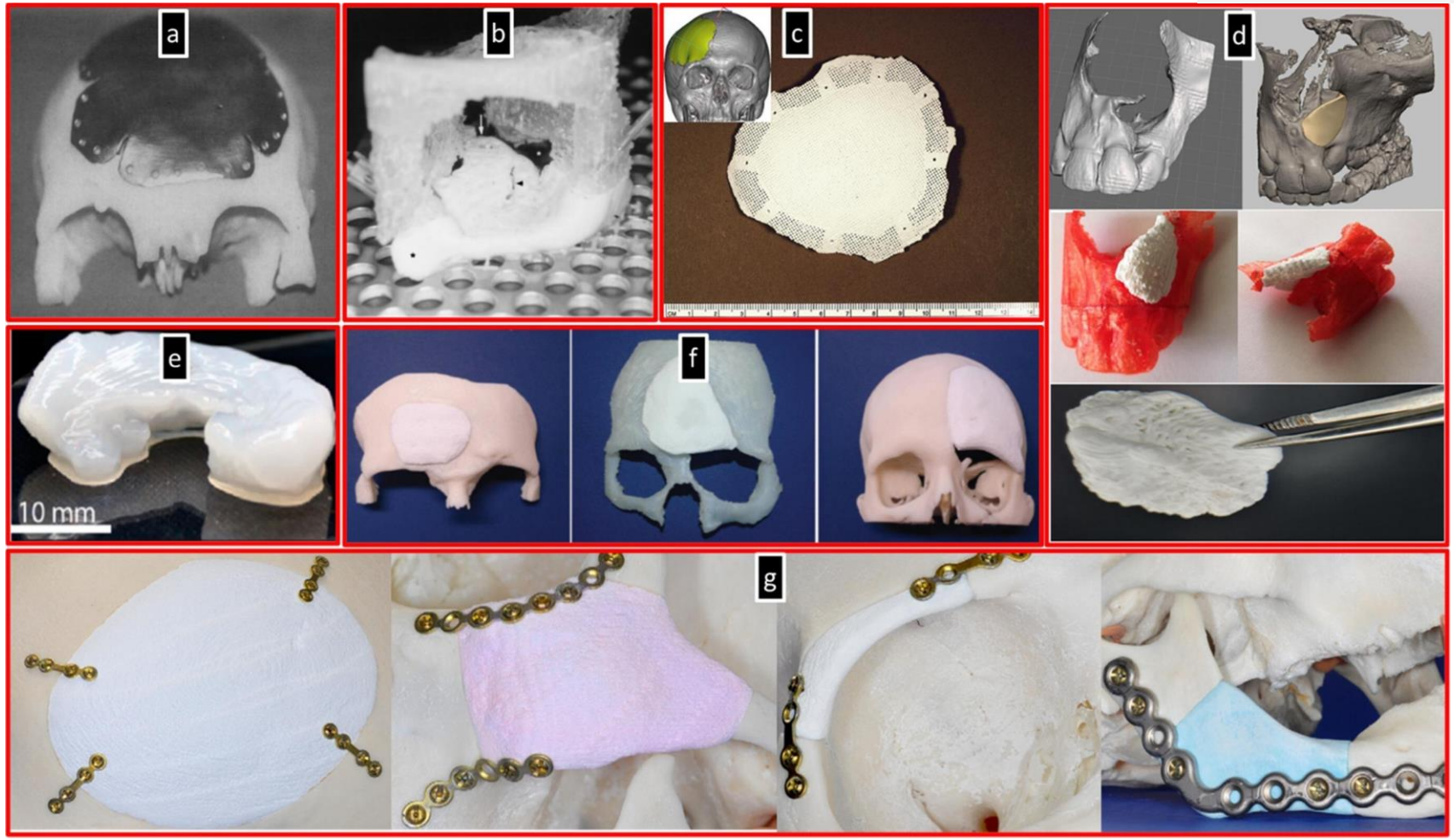

Various biomaterial/AM process couples found in the literature for printing personalized implants. a) titanium/SLS process b) Hydroxyapatite/SLA process c) Hydroxyapatite/SLA process d) Calcium phosphate cement/extrusion-based process e) Hydrogel of alginate/extrusion-based process f) Calcium phosphate cement/powder bed process g) Calcium phosphate cement/powder bed process

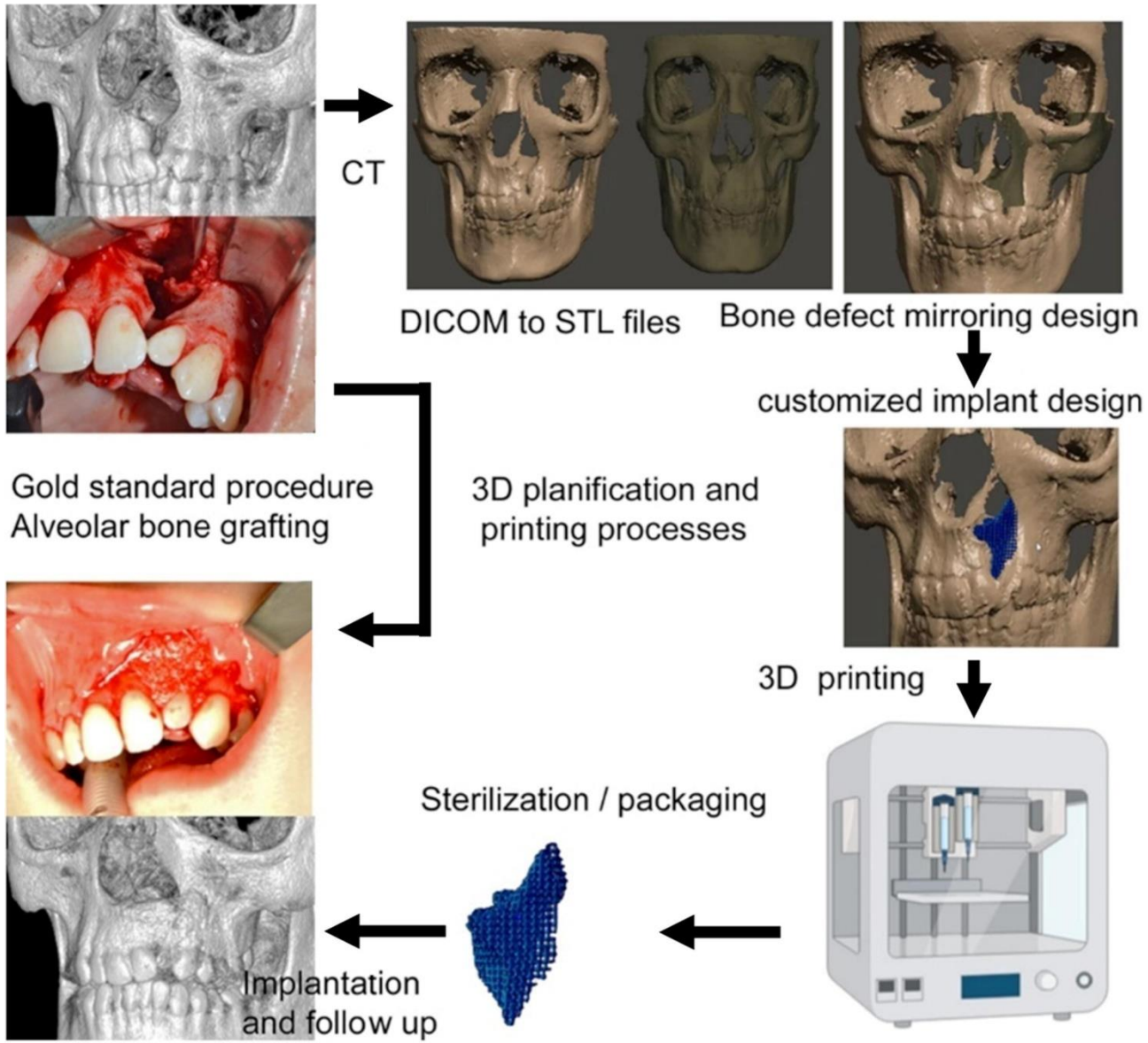

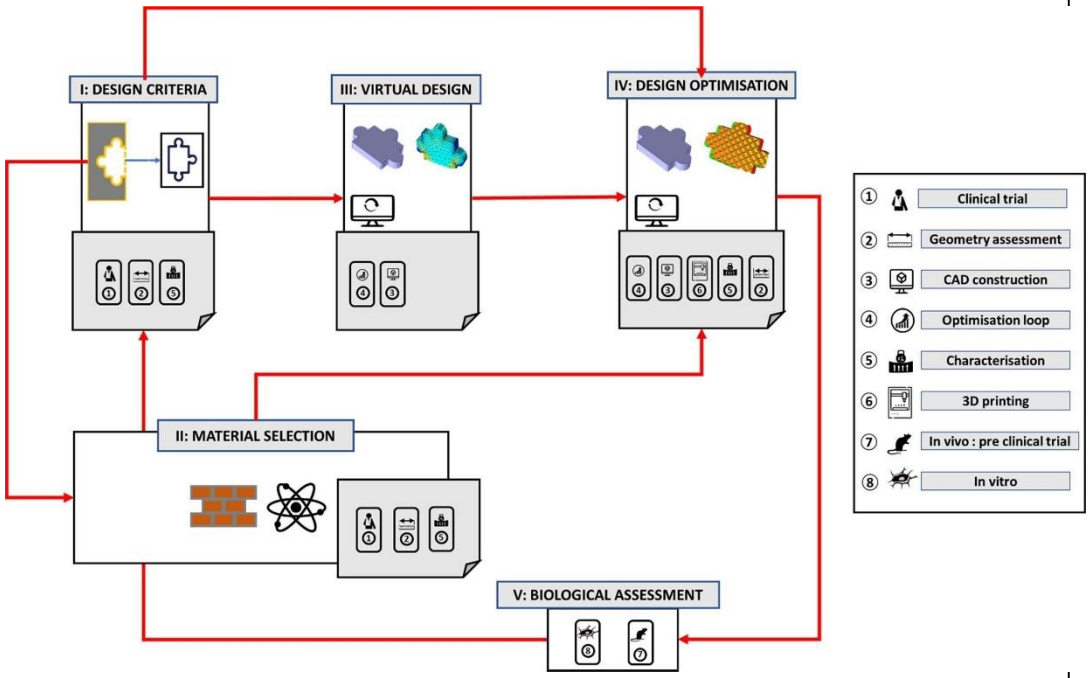

Progress in Materials Science 130 (2022) 100963

Contents lists available at ScienceDirect

Progress in Materials Science

journal homepage: www.elsevier.com/locate/pmatsci

Additive manufacturing of biomaterials for bone tissue engineering – A critical review of the state of the art and new concepts

Marie-Michèle Germaini [a], Sofiane Belhabib [b], Sofiane Guessasma [c], Rémi Deterre [b], Pierre Corre [a], Pierre Weiss [a,*]

3 D microporous controlled structures

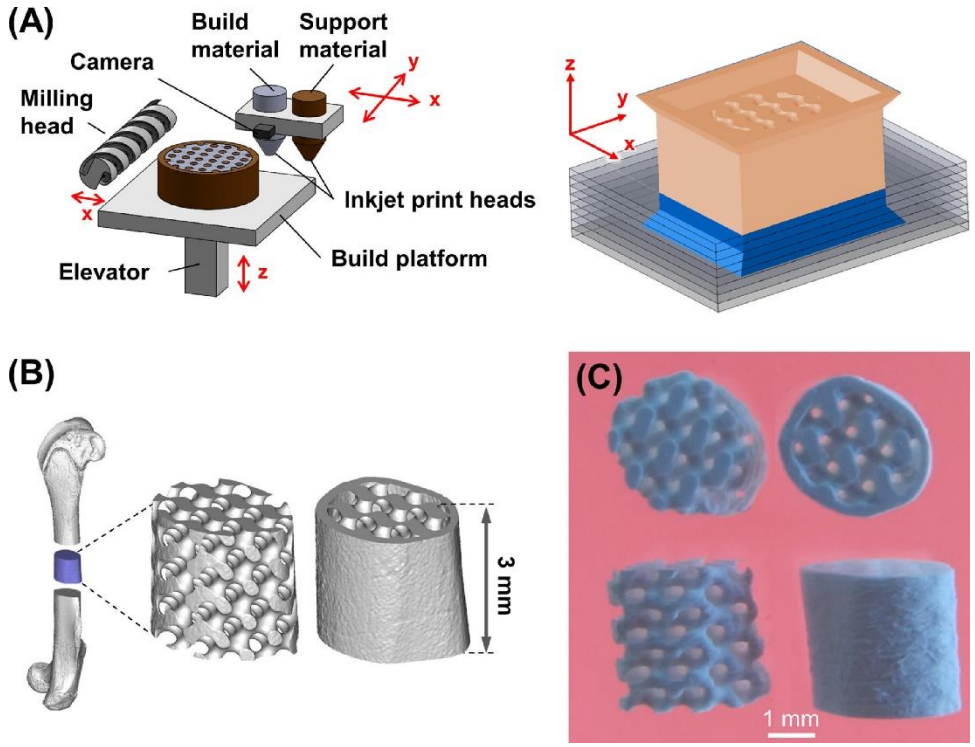

- Printing of 3D Wax mold
- CaP slurry before Sintering
- Gyroid porosity structure without GP or with cortical like outer shell GPRC
- Implanted in a rat femur (8 weeks)

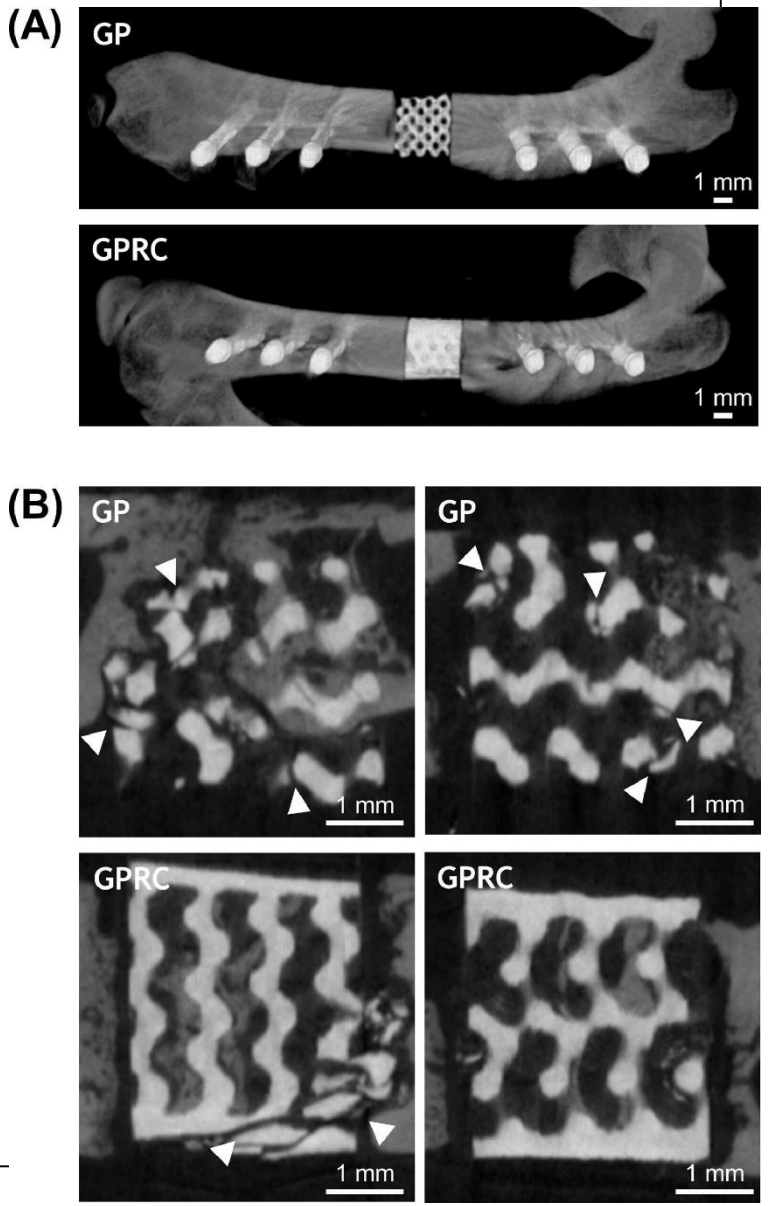

Acta Biomaterialia 109 (2020) 254–266

Contents lists available at ScienceDirect

Acta Biomaterialia

journal homepage: www.elsevier.com/locate/actbio

Full length article

Custom-made macroporous bioceramic implants based on triply-periodic minimal surfaces for bone defects in load-bearing sites

Baptiste Charbonnier[a], Mathieu Manassero[b,c], Marianne Bourguignon[b,c], Adeline Decambron[b,c], Hanane El-Hafci[b,c], Claire Morin[a], Diego Leon[a], Morad Bensidoum[b,c], Simon Corsia[b,c], Hervé Petite[b,c], David Marchat[a], Esther Potier[b,c,*]

ACS Biomaterials SCIENCE & ENGINEERING
Article
Cite This: ACS Biomater. Sci. Eng. 2020, 6, 553−563
pubs.acs.org/journal/abseba

Tailored Three-Dimensionally Printed Triply Periodic Calcium Phosphate Implants: A Preclinical Study for Craniofacial Bone Repair

Arnaud Paré,[†,‡,§,∥,◆] Baptiste Charbonnier,[⊥,◆] Pierre Tournier,[†,∥] Caroline Vignes,[†] Joëlle Veziers,[†] Julie Lesoeur,[†] Boris Laure,[‡,§] Hélios Bertin,[∥,#] Gonzague De Pinieux,[§,▽] Grégory Cherrier,[§,▽] Jérome Guicheux.[†,∥] Olivier Gauthier.[†,∥,○] Pierre Corre.[†,∥,#] David Marchat.[⊥,◆] and Pierre Weiss*[,†,∥,◆]

ACS Biomaterials Science & Engineering
Article

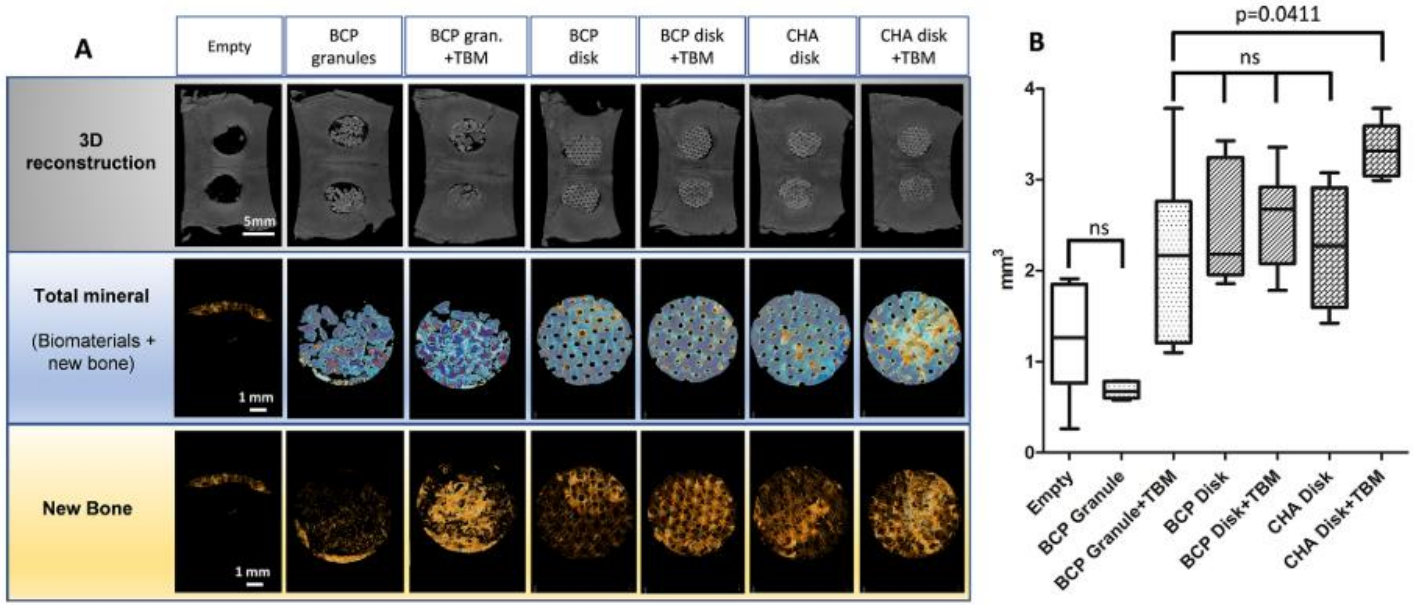

Figure 4. Micro-CT analysis of the critical-sized craniofacial bone defect (CSD) reconstruction. (A) Images of the CSD reconstructions at seven weeks showing calvarial 3D reconstruction, biomaterials + new bone, and newly formed bone alone. CSD repair with BCP granules ± TBM systemically had biomaterial loss and calvarial holes. (B) Graph showing the quantitative analysis of bone volume (BV, mm^3) in the region of interest. Empty defect (negative control) and BCP granule groups had the lowest rate of bone formation compared to others ($p < 0.05$). There was no statistical difference between BCP granules + TBM (positive control) and macroporous disks alone, while the CHA + TBM group had significantly higher bone formation than that of BCP granule + TBM ($p = 0.0441$).

AXIALLY VASCULARIZED CUSTOM-MADE MACROPOROUS BIOCERAMIC FOR RECONSTRUCTION OF SEGMENTAL MANDIBULAR DEFECT: A PRECLINICAL STUDY IN SHEEP

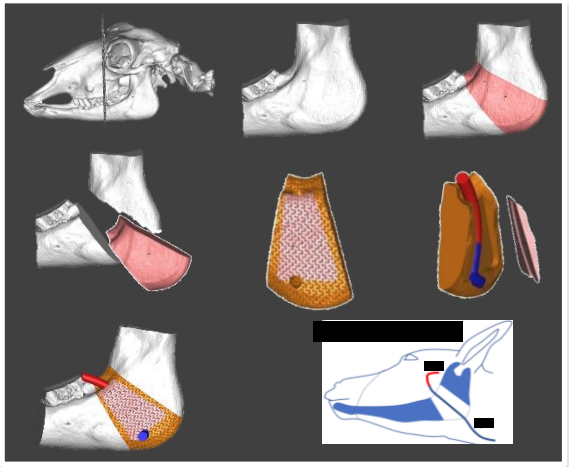

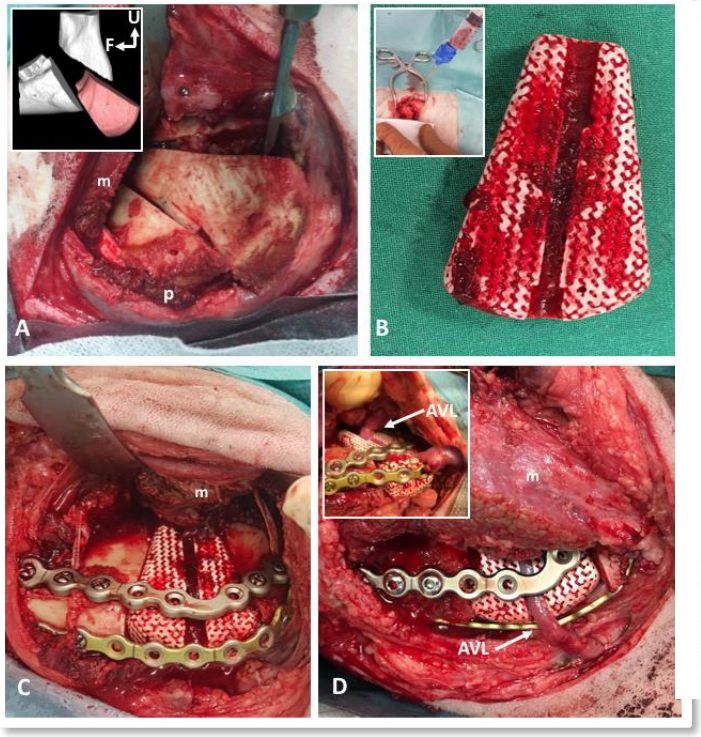

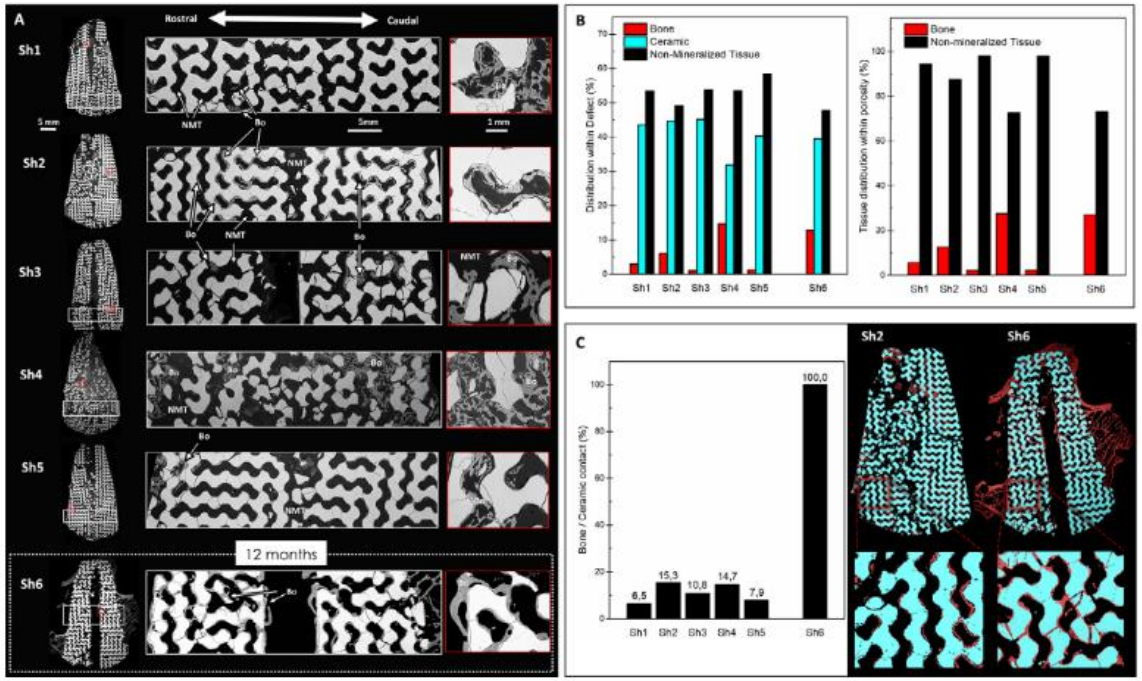

Contents lists available at ScienceDirect

Acta Biomaterialia

journal homepage: www.elsevier.com/locate/actbio

Full length article

Standardized and axially vascularized calcium phosphate-based implants for segmental mandibular defects: A promising proof of concept

Arnaud Paré[a,b], Baptiste Charbonnier[a,c,1], Joëlle Veziers[a], Caroline Vignes[a], Maeva Dutilleul[a], Gonzague De Pinieux[d], Boris Laure[b], Adeline Bossard[e], Annaëlle Saucet-Zerbib[e], Gwenola Touzot-Jourde[a,e], Pierre Weiss[a], Pierre Corre[a,f], Olivier Gauthier[a,e], David Marchat[c,a]

Without polymer or hydrogel **cement is a fragile material**

Additive Manufacturing

- Hopes for a very soon application
  - More and more startups & manufacturers
  - FDA/C€ certification

Ossiform
We Print Bone™

CERHUM

mimetis
Naturally Inspired Bone Regenerative Solutions

ADMATEC

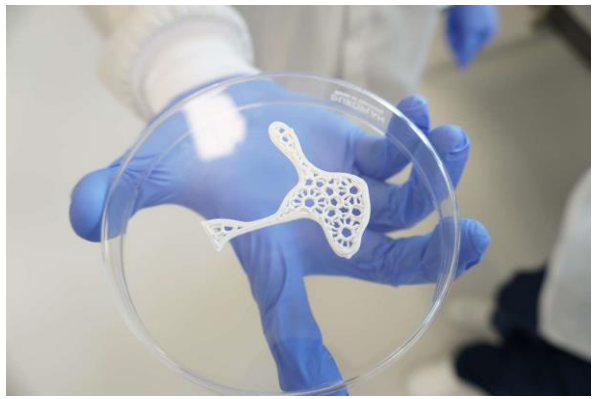

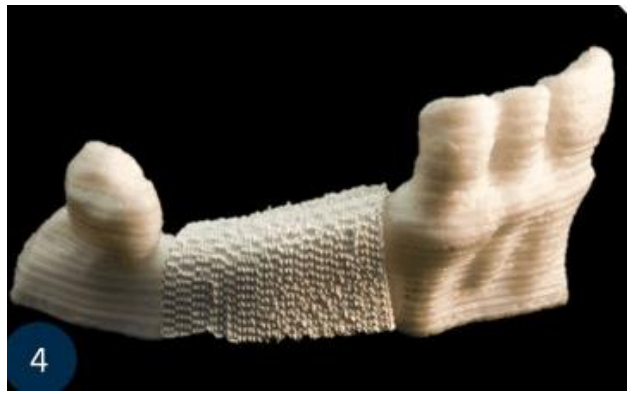

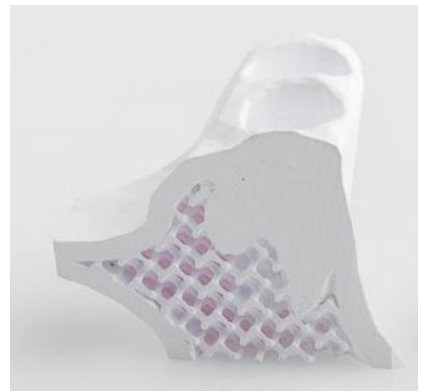

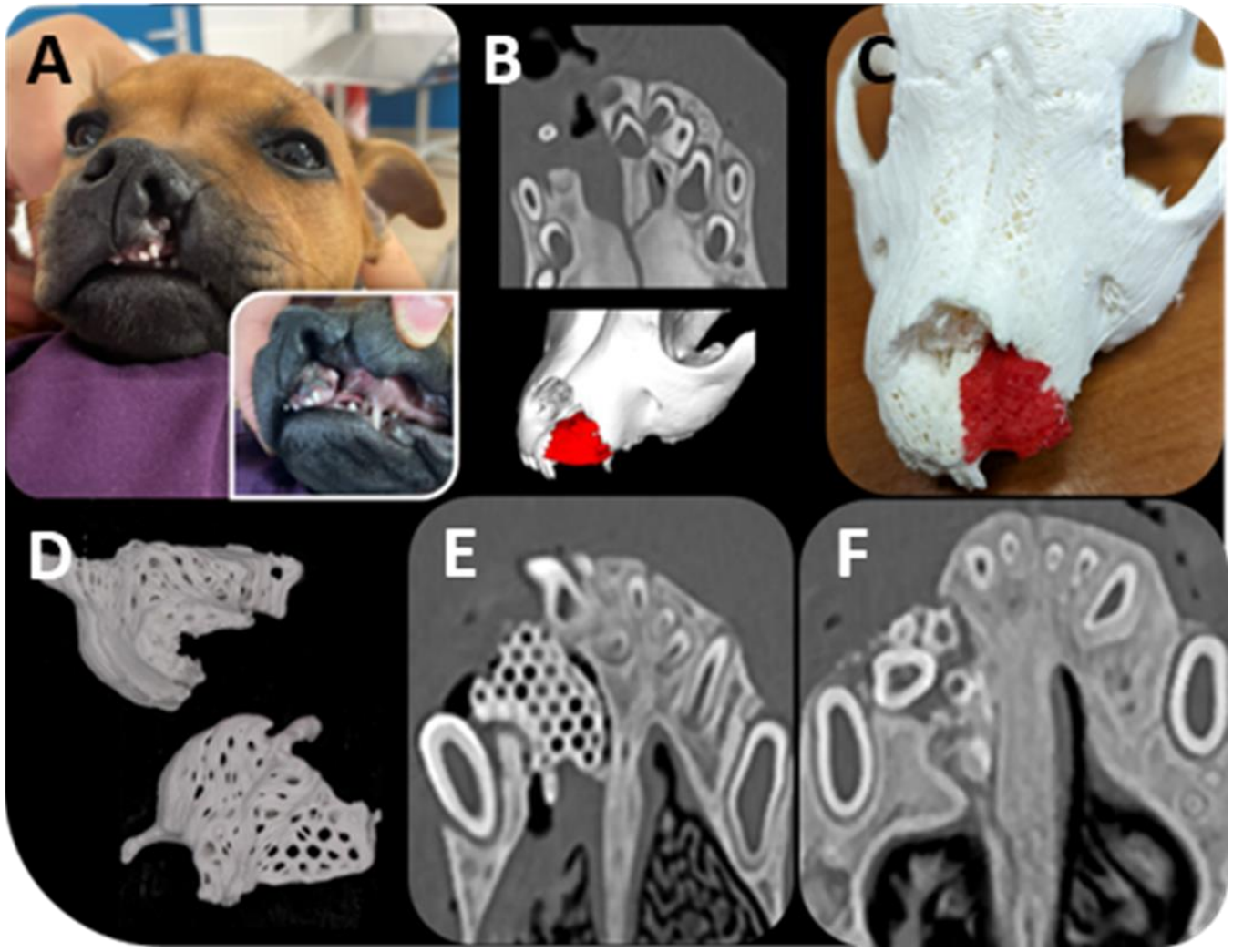

Traitement personnalisé d'un patient chien comportant (A) une fente labiopalatine unilatérale, (B) le scanner préopératoire 2 semaines avant intervention et la conception d'un implant sur mesure (C) la simulation de la chirurgie via modèles 3D polymères (D) l'implant sur mesure conçu en 2 parties pour faciliter son insertion dans le défaut (E) le scanner post-op après la chirurgie reconstructrice et (F) le scanner à 3 mois post-op, montrant une formation osseuse pouvant supporter l'éruption de dents définitives

→ For tomorrow